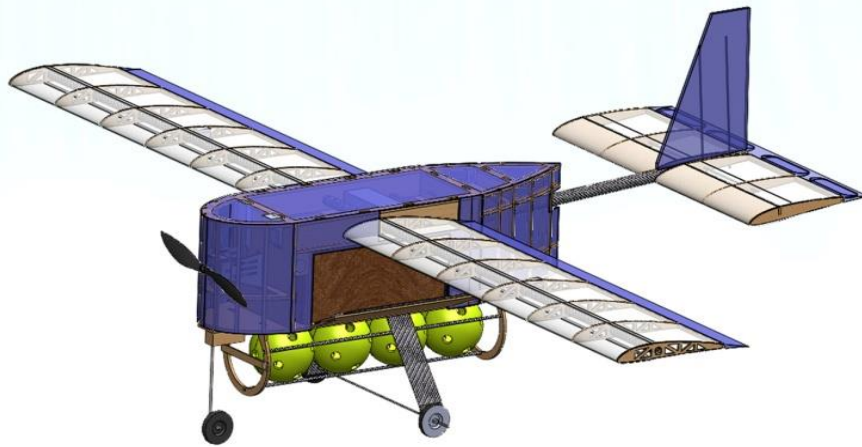




# RASHTREEYA VIDYALAYA COLLEGE OF ENGINEERING

VYOMA



---

**2014-15, AIAA DESIGN/BUILD/FLY REPORT**

---

## Contents

1	EXECUTIVE SUMMARY .....	5
1.1	System Performance.....	6
2	MANAGEMENT SUMMARY .....	6
2.1	Team Organization .....	6
2.2	Milestone Chart .....	7
3	CONCEPTUAL DESIGN.....	8
3.1	Mission Scoring and Requirements .....	8
3.2	Translation into Design Requirements .....	11
3.3	Scoring Sensitivity Analysis.....	12
3.4	Conceptual Design Selection Process .....	14
4	PRELIMINARY DESIGN.....	21
4.1	Design and Analysis Methodology.....	21
4.2	Mission, Constraint and TMS Models.....	23
4.3	Design and sizing trades .....	25
4.4	Propulsion model.....	28
4.5	Lift, Drag and Stability characteristics: .....	30
4.6	Predicted Mission Performance .....	33
5	DETAILED DESIGN .....	34
5.1	Dimensional Parameters .....	34
5.2	Structural Capabilities and Characteristics .....	35
5.3	Systems and Subsystems Design .....	35
5.4	Weights and Balances.....	39
5.5	Flight performance parameters.....	41
5.6	Predicted Mission performance .....	41
5.7	Drawing Package.....	41
6	MANUFACTURING PLAN AND PROCESS.....	46
6.1	Manufacturing and Material Selection.....	46
6.2	Subsystem Manufacturing.....	47
6.3	Structural Integration .....	49
6.4	Prototype Evolution.....	50
6.5	Manufacturing Milestone chart.....	51
7	TESTING PLAN .....	51
7.1	Testing Objectives.....	51

7.2	Propulsion Testing .....	51
7.3	Structural testing .....	52
7.4	Ground Mission Test.....	53
7.5	Payload Drop Testing.....	54
7.6	Flight testing .....	54
7.7	Planned Testing Schedule.....	54
7.8	Pre-flight Checklist.....	55
8	PERFORMANCE RESULTS.....	56
8.1	Propulsion.....	56
8.2	Structure.....	56
8.3	Flight performance .....	57
9	REFERENCES .....	59

## Acronyms and Symbols

<b>AIAA</b>	American Institute of Aeronautics and Astronautics	<b>RVCE</b>	Rashtreeya Vidyalaya College Of Engineering
<b>DBF</b>	Design Build Fly	<b>FOM</b>	Figures of Merit
<b>alpha</b>	Angle of Attack	<b>N<sub>Laps</sub></b>	Number of laps flown
<b>AVL</b>	Athena Vortex Lattice	<b>TMS</b>	Total Mission Score
<b>NiMH</b>	Nickel Metal Hydride	<b>S</b>	Plan form Area
<b>C<sub>p</sub></b>	Power Coefficient	<b>C<sub>t</sub></b>	Thrust Coefficient
<b>rpm</b>	Rotation Per Minute	<b>Q</b>	Torque
<b>OD</b>	Outer Diameter	<b>ID</b>	Inner Diameter
<b>C<sub>f</sub></b>	Skin Friction Coefficient	<b>C<sub>Lmax</sub></b>	Maximum Lift Coefficient
<b>C<sub>hm</sub></b>	Hinge Moment	<b>C<sub>β</sub></b>	Lateral Stability Coefficient
<b>C<sub>nβ</sub></b>	Directional Stability Coefficient	<b>I<sub>0</sub></b>	Motor Idle Current
<b>Tx</b>	Transmitter	<b>Rx</b>	Receiver
<b>FEA</b>	Finite Element Analysis	<b>CA</b>	Cyanoacrylate
<b>RAC</b>	Rated Aircraft Cost	<b>C<sub>D</sub></b>	Drag Coefficient
<b>R/C</b>	Remote Controlled	<b>Re</b>	Reynolds Number
<b>C<sub>Dmin</sub></b>	Minimum Drag Coefficient	<b>GA</b>	Genetic Algorithm
<b>AHP</b>	Analytical Hierarchy Process	<b>C<sub>D0</sub></b>	Parasite Drag Coefficient
<b>CG</b>	Centre of Gravity	<b>C<sub>L</sub></b>	Lift Coefficient
<b>C<sub>Dmin</sub></b>	Minimum Drag Coefficient	<b>C<sub>m</sub></b>	Moment Coefficient
<b>N_Servo</b>	Number of Servos	<b>TOGW</b>	Take -Off Gross Weight
<b>GS</b>	Ground Score	<b>FS</b>	Flight Score
<b>M<sub>1</sub></b>	Mission1 Score	<b>M<sub>2</sub></b>	Mission2 Score
<b>M<sub>3</sub></b>	Mission3 Score	<b>EW<sub>1</sub></b>	Empty Weight in Mission1
<b>EW</b>	Empty Weight	<b>EW<sub>2</sub></b>	Empty Weight in Mission2
<b>EW<sub>3</sub></b>	Empty Weight in Mission3	<b>L</b>	Lift
<b>D</b>	Drag	<b>g</b>	Constraint Variable
<b>g<sub>U</sub></b>	Constraint Upper Limit	<b>g<sub>L</sub></b>	Constraint Lower Limit

## 1 EXECUTIVE SUMMARY

This report documents the design, testing and manufacturing techniques of Rashtreeya Vidyalaya College of Engineering (RVCE), Bengaluru, India in preparation for the 2014-2015 AIAA/Cessna/Raytheon Design/Build/Fly competition held at Tucson, Arizona. RVCE is debuting at this year's event. The problem statement has proven to be challenging in all aspects, bringing the best out of the team. The team also considers it a personal accomplishment to complete the design and fabrication with limited funding and resources. On the whole, it has been an enriching experience for the team.

The theme of this year's competition is to develop a Remote Sensor Delivery and Drop System with the objective of the competition being to produce an electric remote controlled aircraft that will receive the highest Overall Score, which is a combination of the Written Report Score, Total Mission Score and Rated Aircraft Cost (RAC).

The designed aircraft should be capable of completing three flight missions and one ground mission. The objective of the ground mission is to complete payload loading in the least possible duration. The first flight mission is to fly the maximum number of laps possible within 4 minutes, without any payload. The second flight mission is to complete three laps with three wooden blocks (Total Size: 4.5" x 5.5" x 10"; Total Weight: 5 lb.) in the shortest time possible. The third flight mission is to carry as many Champro balls as possible externally and drop one ball per lap in the designated drop zone. Take-off distance was limited to a maximum of 60 feet for each of the flight missions.

Through Scoring Analysis, the team inferred that maximum Overall Score would be attained when all the missions would be completed by an aircraft with least RAC, which is a function of empty weight and number of servos. While RAC was found to be the most important scoring factor in the competition, it is also essential that the aircraft must not compromise on the contribution of each mission towards the Overall Score. The Ground Score, being a relative factor and a direct multiplier, has an equally high priority. Upon thorough analysis, the team came to the conclusion that, out of the three missions, mission 3 has the highest impact on score, while mission 2 has the least. The inverse relation between the number of balls and Ground Mission Score is considered, and the number of balls is optimized to obtain maximum Overall Score.

Aircraft configuration was selected in the conceptual design phase, with the employment of Analytical Hierarchy Process. Through Figures of Merit (FOM) Analyses, the final configuration in each of the subsystem was finalized. The chosen configuration was the Conventional aircraft with tricycle landing gear, single tractor propulsion system, high wing configuration and conventional tail.

To obtain a preliminary design of the aircraft, the team wrote a Genetic Algorithm (GA) based optimization program. This provided a starting point towards the final design of the aircraft.

Detailed design addressed the challenges posed by the ground and flight missions. Ground Mission tested the robustness and simplicity of the payload loading mechanisms. The first flight mission tested the speed and handling characteristics of the aircraft. This was tackled by opting for a high pitched propeller. The second flight mission determined how capable the aircraft was, in carrying the given payload. In order to satisfy 60-ft limit on Take-Off Distance, flaps were employed. Mission 2 payload was secured using foam and neodymium magnets. The third flight mission tested the simplicity and reliability of the dropping mechanism employed. Carbon rod rails were used to secure the balls externally and actuation of servo would ensure the drop of one ball each lap.

Meticulous planning and execution of manufacturing processes and flight tests helped the team to adopt an iterative approach to optimize the aircraft design. The team formulated a strategy for each of the phases in the build up towards the competition. This is indicated by flowcharts throughout the report.

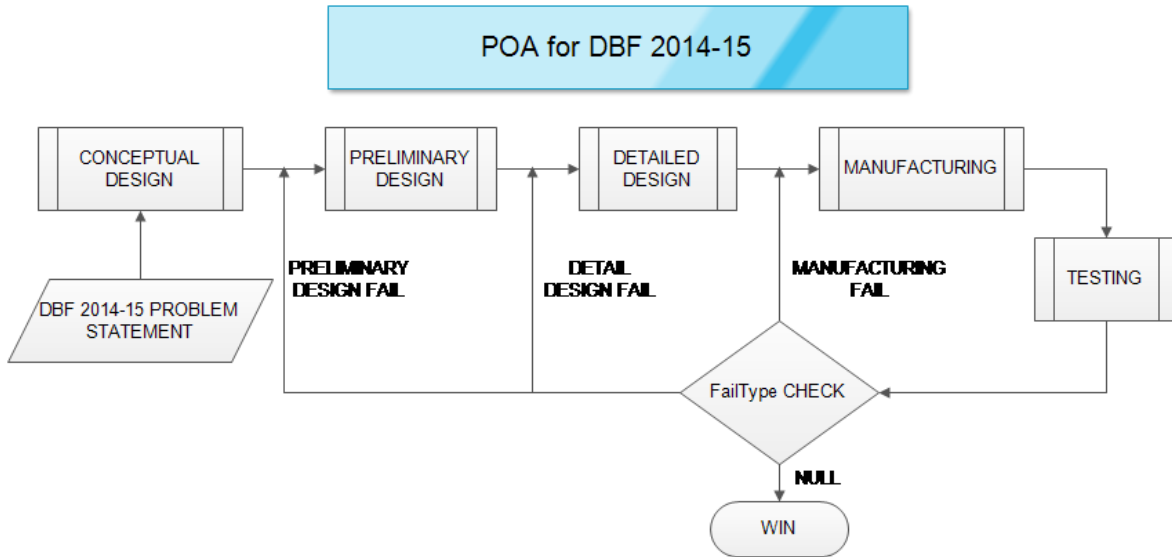


Figure 1.1: RVCE’s Plan of Action (POA) to win AIAA DBF 2014-15 Competition.

## 1.1 System Performance

The ground mission of loading and unloading payloads could be completed within 20 seconds. A maximum of 6 laps could be completed in Mission 1. While carrying Mission 2 payload, three laps can be completed in little over two minutes. Four balls can be dropped, one per lap completed, while attempting for mission 3. With a quick-fire loading time and a lightweight design, the team is confident of having delivered a very competitive design.

## 2 MANAGEMENT SUMMARY

The 2014-2015 RVCE DBF team consists of 11 students, all being juniors, operating on a co-curricular basis. In an effort to optimize the workforce, the team members were in charge of one technical and one managerial role. The team implemented an organizational structure for both domains, which ensured effective distribution of workload. Though the focus was always on excelling in the competition, the vision was to gain knowledge and experience in the field of aerospace, which has been a common interest among the members of the team.

### 2.1 Team Organization

Although the team consisted of juniors alone, a structure was established to ensure accountability and efficient work distribution. The distribution was based on skill and interests. Many members contributed to multiple subsystems, however for the sake of convenience, each subsystem had a point of contact. The hierarchical chart below shows members under the subsystems in which they made the largest contributions.

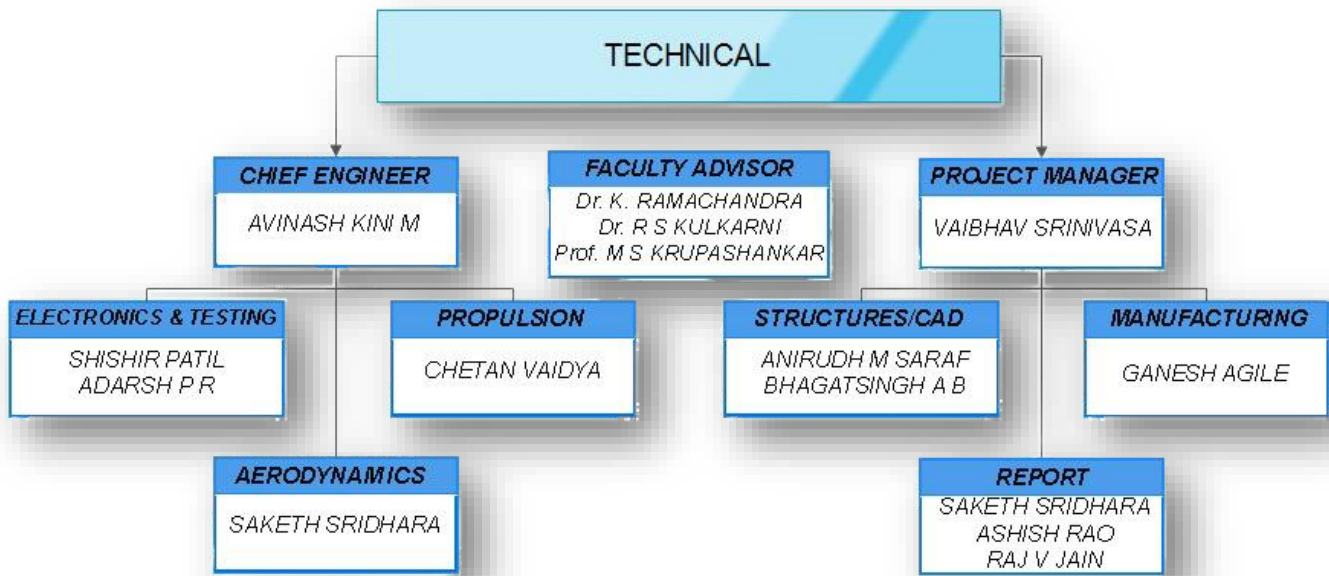


Figure 2.1: Technical Organization Chart

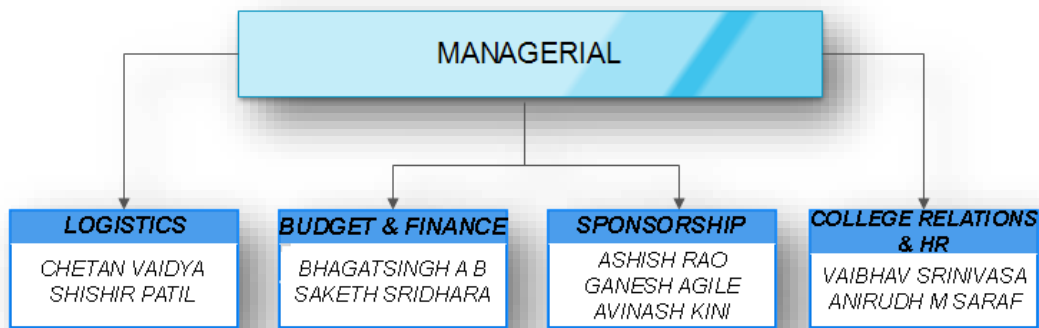


Figure 2.2: Managerial Organization Chart

## 2.2 Milestone Chart

It was extremely important to stay on a reasonable schedule to meet the deadlines for report and competition. A Gantt chart detailing the planned and actual durations is demonstrated below. Though the deadlines set internally by the team are fluid, they were expected to be met with quality and finished work. Since this was a new type of challenge, the team considers this as a learning curve, and this year's shortcomings serve as valuable inputs to the future years.

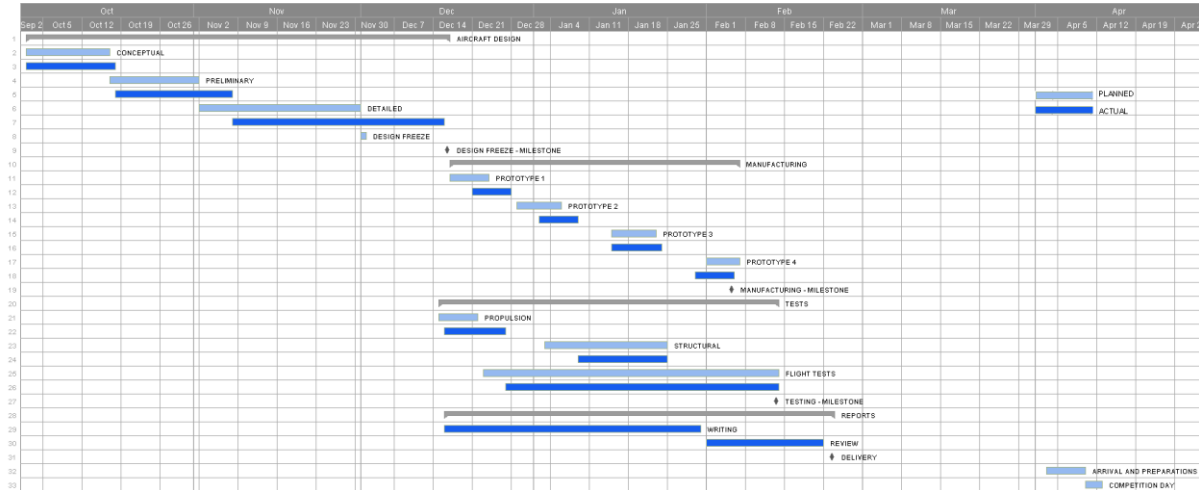


Figure 2.3: 2014-2015 RVCE DBF Milestone Chart

### 3 CONCEPTUAL DESIGN

Conceptual design aids in selecting the best aircraft configuration based on the mission requirements, enabling the aircraft to achieve highest possible Overall Score. The score sensitivity analysis conveys the most important parameters in the scoring equation, which serves as a basis for making design related choices. Analytical Hierarchy Process (AHP) provides accurate normalized weightage to the design requirements in the configuration selection matrix.

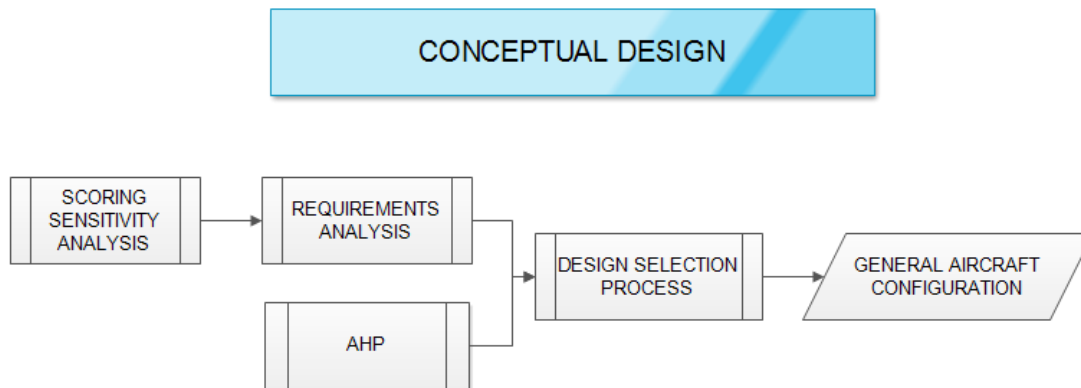


Figure 3.1: Conceptual Design Flowchart

#### 3.1 Mission Scoring and Requirements

The 2014-15 AIAA Design/Build/Fly (DBF) competition comprises four aircraft missions: One ground mission and three independent flight missions. Each of these missions test different capabilities of the aircraft and contribute to the Overall Competition Score.

##### 3.1.1 Aircraft requirement and constraints

- Maximum of 5 minutes are provided to load the payload and verify the aircraft systems as fully functional.
- The weight of the battery pack(s) should not exceed **2.0 lb**.
- Only off the shelf NiCad or NiMH batteries can be used.
- Motors and batteries may be limited in current draw by means of a fuse.



- The aircraft TOGW (take-off gross weight with payload) should not exceed 55 lbs.
- The aircraft must be able to take off within 60ft in all missions.
- The aircraft fuselage should be capable of accommodating a 5lb payload of dimensions 4.5" x 5.5" x 10".
- All aircraft radios must have a fail-safe mode that is automatically selected during loss of transmit signal.
- All aircraft must have a mechanical motor arming system separate from the on-board radio Rx switch
- Aircraft must land successfully at the end of each mission for the mission to receive a score.

### 3.1.2 Flight Lap

The standard flight lap is shown in figure 3.2. A successful lap demands

1. Rolling take off in less than 60 feet
2. Climb to safe altitude
3. U-turn 500 feet upwind of start
4. 1000 foot downwind leg with a 360 degree turn away from the runway
5. 180 degree turn from downwind to upwind
6. 500 foot upwind past the start line

And at the end of each mission, successful landing is essential to obtain the score.

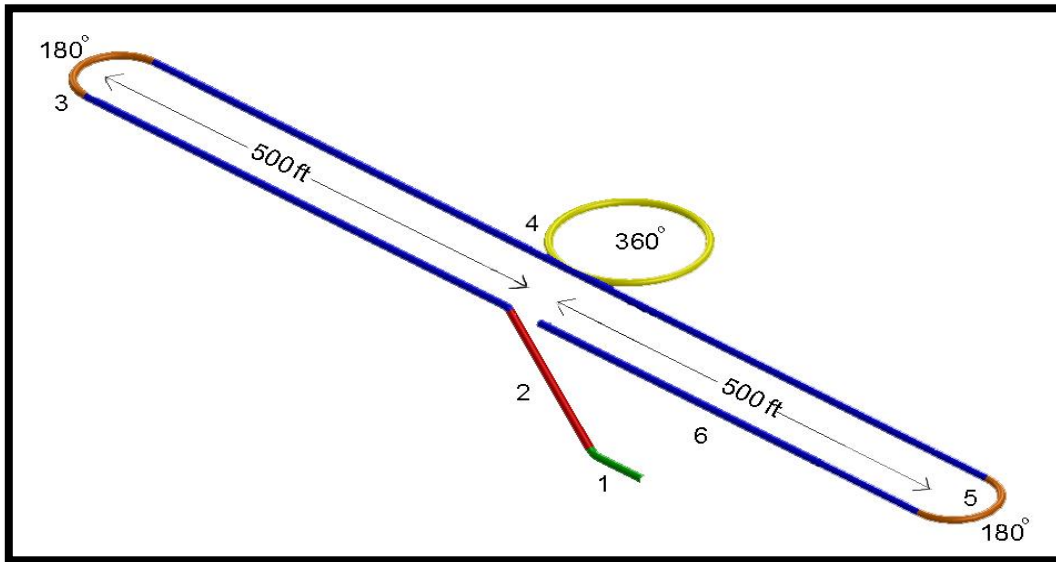


Figure 3.2: Competition Flight Course

### 3.1.3 Scoring

The team's score will be determined by the following formula:

$$\text{Overall\_Score} = \text{Written\_Report\_Score} * \frac{\text{Total\_Mission\_Score}}{\text{RAC}} \quad (\text{Eq. 3.1})$$

The Total Mission Score is the product of the Ground Score (GS) and Flight Score (FS):

$$\text{Total\_Mission\_Score} = \text{GS} * \text{FS} \dots \dots \dots (\text{Eq. 3.2})$$

The flight score is the sum of the individual mission scores:

$$\text{Flight\_Score} = FS = M_1 + M_2 + M_3 \text{ (Eq. 3.3)}$$

The RAC is a function of empty weight and complexity:

$$RAC = EW * N\_Servo \text{ (Eq. 3.4)}$$

Empty weight will be measured after each successful scoring flight:

$$EW = \max(EW_1, EW_2, EW_3) \text{ (Eq. 3.5)}$$

### 3.1.4 Missions:

#### Ground Mission - Payload Loading Time

Ground mission starts with the aircraft empty and hatches closed. As soon as the timing is commenced, three team members are allowed to load and secure mission 2 payload. The crew leaves the loading area and time is paused to verify if the aircraft is secure. Timing is resumed following which the mission 2 payload is removed and mission 3 payload is installed. The hatch door is closed again and the crew leaves the area. Time is brought to a stop. It is essential that the mission be completed within five minutes from the start of timing. The mission score is given by:

$$GS = \frac{\text{Loading\_Time}_{\text{Fastest}}}{\text{Loading\_Time}_{\text{VYOMA}}} \text{ (Eq. 3.6)}$$

#### Flight Mission 1 - Ferry Flight

The first mission is a ferry flight mission requiring the aircraft to complete as many laps as possible within a 4 minute flight time. Timing starts when the throttle is advanced for take-off. M1 score is defined by equation

$$M_1 = 2 * \frac{N_{\text{Laps}_{\text{VYOMA}}}}{N_{\text{Laps}_{\text{Max}}}} \text{ (Eq. 3.7)}$$

#### Flight Mission 2 - Sensor Package Transport Mission

The second mission is a sensor package transport mission. It is essentially a three lap mission with sensor package secured internally, the sensor package consists of one stack of three standard 2 x 6 wooden pine boards of length 10". The nominal overall size is 4.5" x 5.5" x 10" and the nominal weight is 5lb. The aircraft must land successfully to receive a score for the mission. The scoring criterion is given in equation below.

$$M_2 = 4 * \frac{\text{Time}_{\text{Fastest}}}{\text{Time}_{\text{VYOMA}}} \text{ (Eq. 3.8)}$$

### Flight Mission 3 - Sensor Drop Mission

The third mission is a sensor drop mission. It consists of 12" circumference Champro Balls as the payload. During each lap the plane should remotely drop a single Champro Ball at the pre-designated "drop zone". A lap will only count if a single ball is dropped within the drop zone. Multiple drops in the zone in a single lap will invalidate that lap. Mission 3 score is given by the equation:

$$M_3 = 6 * \frac{N_{Laps_{VYOMA}}}{N_{Laps_{Max}}} \text{ (Eq. 3.9)}$$

### 3.2 Translation into Design Requirements

The competition rules and scoring requirements were translated into qualitative design metrics that could be used to evaluate and choose an aircraft configuration.

Table 3.1: Translation into Design Requirements

SL. NO.	MISSION REQUIREMENTS	DESIGN REQUIREMENTS
<b>General Aircraft Requirements</b>		
1	Battery weight must not exceed 2-lb.	Power requirements to be optimized for each mission.
2	RAC is a function of empty weight and number of servos	<ul style="list-style-type: none"> <li>Simplify and justify each component of aircraft.</li> <li>Optimized wing area for max lift and minimum weight.</li> </ul>
3	All payloads must be secured	Integrate restraint systems with aircraft structure.
4	Aircraft must use ground rolling take-off within 60 ft.	<ul style="list-style-type: none"> <li>Powerful propulsion system.</li> <li>Critical wing area required.</li> <li>Appropriate landing gear configuration to ensure safe landing</li> </ul>
<b>Ground Mission</b>		
5	Assembly and loading of payload within 5 minutes by 3 team members	Loading mechanism must be simple yet robust.

Mission 1		
6	4 minute flight	Propulsion system optimization
7	Scored on number of complete laps	<ul style="list-style-type: none"> <li>• High velocity.</li> <li>• Aerodynamic Design to reduce drag.</li> <li>• High maneuverability for sharp turning</li> </ul>
Mission 2		
8	Fly 3 laps, timed	High velocity and high maneuverability with given payload
9	Internal Payload:5 lbs.	Maximize payload fraction
Mission 3		
10	Fly with team selected number of Champro balls	<ul style="list-style-type: none"> <li>• Optimize number of balls and loading time.</li> <li>• Position payload accurately to minimize drag</li> </ul>
11	Drop one Champro ball per lap	<ul style="list-style-type: none"> <li>• Plane design for dynamic CG.</li> <li>• Reliable dropping mechanism</li> </ul>

### 3.3 Scoring Sensitivity Analysis

An ideal aircraft should maximize the TMS by being the best performer in each of the three missions. However, each mission individually tests different capabilities of the aircraft. It is a challenge to improve the performance specifically in one mission alone, without negatively affecting the performance in the other mission(s) or the parameters that comprise the scoring equation. Scoring sensitivity analysis is conducted to determine the most influential parameter, based on the following equation.

$$Total\_Score(Excluding\ Report\ Score) = \frac{Total\_Mission\_Score}{RAC} \quad (Eq. 3.10)$$

$$Total\_Score(Excluding\ Report\ Score) = \frac{2 * \frac{N_{Laps_{VYOMA}}}{N_{Laps_{Max}}} + 4 * \frac{Time_{Fastest}}{Time_{VYOMA}} + 6 * \frac{N_{Laps_{VYOMA}}}{N_{Laps_{Max}}}{EW * N_{Servo}} \quad (Eq. 3.11)$$

Figure 3.3 shows the percentage change in total score as a function of a percentage change in a single score variable on the X-Axis. The origin (0, 0) represents the baseline aircraft performance, and any variation is a percentage change in its scoring parameters.

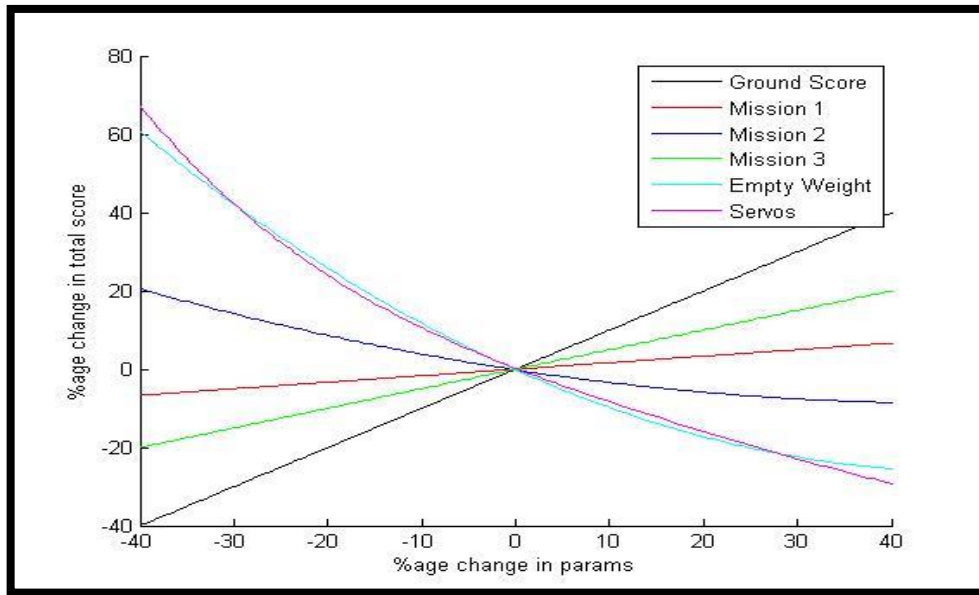


Figure 3.3: Scoring Sensitivity Analysis

Table 3.2: Baseline Aircraft Data

BASELINE AIRCRAFT DATA	
#Laps	5
Time for Mission 2 (s)	125
#Balls	5
#Servos	5
Empty Weight (lbs)	4.4

The analysis is conducted based on baseline aircraft data, which enables the team to study the trends and signify the importance of the parameters involved in the scoring equation. Baseline data was obtained from the previous editions of the event and certain calculated guesses. Parameters with greater magnitude of slope in figure 3.3 have the greatest impact on the total score. It can thus be inferred that RAC and GS are the most influential parameters, then followed by 3<sup>rd</sup> mission score.

The ground mission requirement adds a human factor to the overall score. Therefore, the team also emphasized on practice and simplicity of the mechanism involved. The team gained a conceptual grasp of the ergonomics and structural requirement of payload loading.

### 3.4 Conceptual Design Selection Process

At every point in the system design, Analytical Hierarchy Process (AHP) [7] based trade-off analysis was conducted to narrow-down on the appropriate sub-system and reduce the solution space.

The Analytical Hierarchy Process (AHP) is a systematic method for comparing a list of alternatives. A set of comparison criteria known as the requirements or Figures of Merit (FOMs) are first established. The AHP trade-off is then initiated by assigning weightage to the requirements relative to each other in a matrix, and then normalizing it. This provides the Normalized weighting factors for each of the requirements. All the alternatives are then assigned weights relative to each other for the respective requirements. The summation of the product of nominal weights and the weights assigned to each alternative results in the total points for that alternative. The best alternative is the one with the highest total points. Table 3.3 shows the alternatives considered for configuration selection.

Table 3.3: Complete Matrix of Alternatives

COMPONENTS		ALTERNATIVES		
Wing Layout		Conventional	Flying Wing	Bi-Plane
Wing Position		Low wing	High wing	
Tail Configuration		Conventional	T-Tail	V-Tail
Motor Configuration		Pusher	Tractor	
Landing Gear		Bicycle	Tail dragger	Tricycle
Payload Mechanism	Mission 2	Plastic stoppers	Neodymium magnets	
	Mission 3	Rails	Strings	

#### 3.4.1 Wing Layout

The design process was initiated by selecting the wing layout that took into consideration the results from the scoring analysis. Figures of Merit were used to determine the appropriate design configuration based on previously determined design requirements.

#### Configurations Figures of Merit:

The FOMs were based upon the team's past experience and current manufacturing capability. The scoring parameters were-



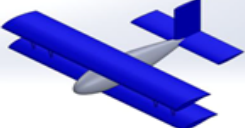
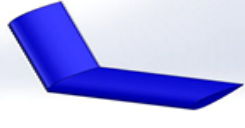
- **Empty Weight-** Aircraft's empty weight is the most crucial component of the Total Score since it strongly affects both RAC as well as mission score.
- **Lift to Drag Ratio-** This was given the second highest weightage as it can be directly linked to flight performance.
- **Assembly-** This factor concerns the ease with which the payload can be loaded in the fuselage, which is a significant parameter in the Ground Mission.
- **Cruise velocity-** High cruise velocity ensures quicker laps, thereby enhancing the flight mission scores.
- **Manufacturability/Repairability-** The ease with which the aircraft can be manufactured and repaired was a consideration in the design process. Complex designs require more time to build, and also increase repairing time. Hence the aircraft should be simplistic in design.

- **Number of Servos-** The total number of servos in the selected configuration must be minimal in order to reduce RAC.
- **Handling-** A stable and easy to fly aircraft is essential to complete the flight course

### Configurations Considered

- **Flying Wing-** Without fuselage, this configuration has little potential to carry a high volume internal payload. Manufacturing is relatively complex. Though the drag is greatly reduced, they are generally less stable because of the lack of Horizontal Stabilizer. They also lead to an increased take off distance.
- **Bi-Plane-** Bi-plane increases the empty weight due to the additional wing. They allow a shorter wingspan at the expense of increased drag.
- **Conventional-** Often used in large payload applications, an extensive knowledge base is available. This configuration involves simple and reliable fabrication technique. Easy to design and provides the most design flexibility.

Table 3.4: Aircraft Configuration Decision Matrix

				
		Conventional	Bi Plane	Flying Wing
Requirements	Norm Weighting	Norm Rating	Norm Rating	Norm Rating
Empty Weight	0.24	2	1	3
L/D	0.22	3	2	1
Cruise Velocity	0.14	3	2	1
#Control Surfaces	0.12	2	1	3
Aspect Ratio	0.12	2	1	3
Stall Velocity	0.08	2	1	3
Manufacturability	0.07	3	1	3
Repairability	0.01	3	1	2
<b>Grand Total</b>		<b>2.44</b>	<b>1.36</b>	<b>2.26</b>

Conventional aircraft configuration was chosen because it is generally more stable, has large payload volume in the fuselage and good payload accessibility.

### 3.4.2 Empennage

Based on the chosen monoplane configuration, an empennage was chosen to provide necessary stability and control characteristics while minimizing drag and RAC. The designs considered were Conventional Tail, T Tail and V tail.

- **Conventional Tail** - It consists of a single vertical stabilizer placed on top of a horizontal stabilizer. Horizontal stabilizer and control surface counteract the negative pitching moment of the wing. Vertical stabilizer provides the required longitudinal stability. It is easy to design and build.

- **T Tail** - It is a common variant of conventional tail. Here the horizontal tail is mounted on top of the vertical stabilizer, which allows it to be mounted clear of the wing wake. However, structural weight increases due to the complexity involved in mounting and supporting the horizontal stabilizer.
- **V Tail** - The stabilizers form a V shape, providing both pitch and yaw control. This is easier to integrate than a T Tail, but is still heavier than a conventional one. The advantage of V Tails is the less parasite drag it offers, as the wetted area is less. However, the complexity of control system increases due to the integration of rudder and elevator.

Table 3.5: Stabilizer Configuration Decision Matrix

				
		Conventional	V Tail	T Tail
Requirements	Norm Weighting	Norm Rating	Norm Rating	Norm Rating
System Weight	0.30	2	3	1
#Servos	0.21	3	1	3
Stability & Control	0.15	2	1	3
Manufacturability	0.15	3	2	1
Drag	0.11	2	3	1
Tail Efficiency	0.08	1	3	2
<b>Grand Total</b>		<b>2.28</b>	<b>2.13</b>	<b>1.80</b>


The conventional tail configuration was selected. It is the lightest, easiest to control and fabricate. It also allows the pitch control surface to be located within the prop wash, thus increasing the elevator's effectiveness and thereby improving flight performance.



### 3.4.3 Wing Position

Table 3.6 compares high wing and low wing configurations.

Table 3.6: Wing Position Decision Matrix

			
		High Wing	Low Wing
Requirements	Norm Weighting	Norm Rating	Norm Rating
Stability	0.30	2	1
System Weight	0.22	1	2
Ease of Loading	0.14	1	2
Ease of Dropping	0.14	2	1
Ground Effect	0.10	1	2
Manufacturability	0.10	2	1
<b>Grand Total</b>		<b>1.54</b>	<b>1.46</b>

Based on the results of the comparison, the high wing configuration was selected. It is easier to keep the air flow in front of vertical and horizontal stabilizers clean, as the majority of the fuselage would be below the tail. Although the structural weight of low wing design is less when compared to high wing, the CG in case of low wing designs is above the wing. This could potentially lead to roll instability.


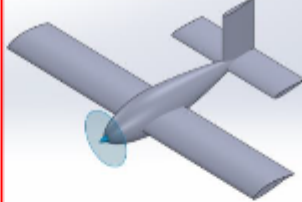
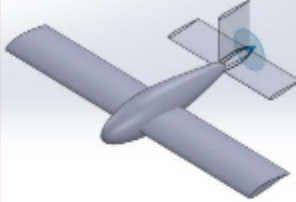
### 3.4.4 Motor Configuration

The Motor configuration selection plays an important role in satisfying take-off criteria. The addition of an extra servo prompted the team to discard the possibility of a twin puller configuration even though it had increased local velocity directly over the wing and flaperons.

After considerable scouting the motor configurations considered were:

- **Single tractor** - This is a lightweight configuration in which the probability of propeller hitting ground on take-off is very less. Forward mounted props have higher efficiency as they act on undisturbed air.
- **Single pusher** - In this configuration, motor is mounted at the rear end of the aircraft which ensures better airflow around the airframe. Also propulsion efficiency is reduced as the propeller acts in the wing wake. Maintaining the position of the CG will be a major challenge as the aircraft tends to be heavier at the tail.

Table 3.8: Motor Configuration Decision Matrix

			
		Single Tractor	Single Pusher
<u>Requirements</u>	<u>Norm Weighting</u>	Nom Rating	Nom Rating
Thrust/Weight	0.30	2	1
Manufacturability	0.20	2	1
Efficiency	0.20	2	1
Weight	0.15	2	2
Stability	0.15	2	1
<b>Grand Total</b>		<b>2.00</b>	<b>1.15</b>

Based on the results of the trade off, single tractor configuration is selected.

### 3.4.5 Payload Mounting Mechanism

Simplicity of payload mounting mechanism is of paramount importance in order to maximize ground score. Mounting procedure must be simple yet robust.

#### Mission 2:

For mission 2, a payload of 5-lb must be secured internally. Thus, ease of access is an essential requirement. The ground mission demanded swift loading and unloading of the payload. Considering this, the team arrived at two feasible hatch-door designs.

One design involved employing stoppers at one end for opening and closing, while the other end is hinged. The second design involves using neodymium magnets instead of plastic stoppers.

Shown below is the comparison between the two available choices.

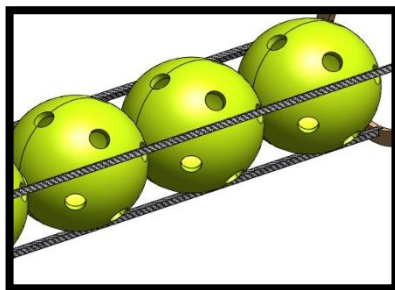
Table 3.9: Payload Door Decision Matrix

					
		Norm Rating	Norm Rating	Norm Rating	Norm Rating
<b>Requirements</b>	<b>Norm Weighting</b>				
Loading & Unloading Time	0.40	1	2	2	1
Weight	0.25	2	1	2	2
Ease of Manufacture	0.20	1	2	2	1
Reliability	0.15	2	1	1	2
<b>Grand Total</b>		<b>1.45</b>	<b>1.75</b>		

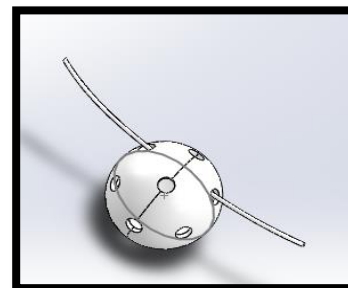
Neodymium magnets design was incorporated, due to its advantages over the plastic stopper. The speed of loading and unloading was the decisive factor of consideration.

**Mission 3:**

For mission 3, Champro balls are to be secured externally, and one ball is to be dropped per lap. The intention is to carry the external payload with minimal drag. Also, these balls have to be located in close vicinity of the CG, for minimal variations in stability. The team hence decided that the optimal location of payload was under the fuselage. The payload sub-team came up with two feasible dropping mechanisms, which make use of a single servo.



(a) RAILS Configuration



(b) STRINGS Configuration

Figure 3.4: Alternatives for External Payload Mounting

The first mechanism involved using rails which run under the fuselage to support the balls as shown in Fig 3.4 a. One ball is dropped from the rear end by the actuation of servo, each lap.

The other one involved the use of string loops which pass through the holes of Champro balls in order to secure them as shown in Fig 3.4 b. Once the servo is actuated, one end of the string is cut loose enabling ball drop.


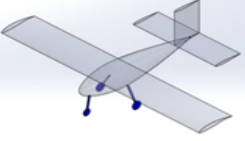
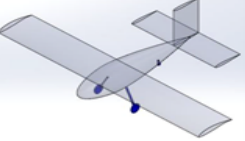
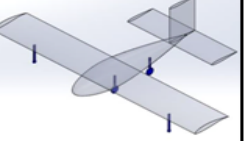
Rail configuration was incorporated into the design, because of the shorter time of loading, ease of manufacture and simplicity. In order to maximize ground score, utmost importance was given to the procedure of unloading the mission 2 payload and simultaneously loading the Champro balls. For speedy execution of the ground mission, the team decided that the payload mounting positions for mission 2 and mission 3 are placed separately so that they can be accessed simultaneously. Further detailed explanation for the payload mounting mechanism is explained later in section 5.3.

### 3.4.6 Landing Gear Configuration

Take-off and landing are critical for the successful completion of the missions. The challenge at take-off is to maintain sufficient control during the ground roll till the aircraft attains the required velocity. The landing gear must be able to withstand impact loads during touchdown. The configurations considered were the following-

- **Tricycle** - In this configuration, two main wheels are under the wing and one smaller wheel is under the nose. This configuration is stable; however the structural weight of this configuration is relatively high.
- **Tail Dragger** - Two main gear wheels are under the wing and one small. This has poor handling during cross winds, however offers less drag when compared to the others.
- **Bicycle** - This configuration has two centerline wheels and two wing tip skids thus faring poorly in ground handling. Also it is very challenging to mount the payload in mission 3.

Table 3.10: Landing Gear Configuration Decision Matrix

				
		Tricycle	Tail Dragger	Bicycle
Requirements	Norm Weighting	Norm Rating	Norm Rating	Norm Rating
Stability	0.27	2	3	1
Empty Weight	0.19	1	2	3
Cross-wind Stability	0.15	3	1	2
Maneuverability	0.13	1	1	3
Take-off Capability	0.12	3	2	1
Manufacturability	0.09	3	2	1
Familiarity	0.05	3	2	1
<b>Grand Total</b>		<b>2.09</b>	<b>1.99</b>	<b>1.79</b>

The Tricycle configuration was selected due to its reliability and superior ground handling ability. Although the structural weight is high, it is best suited for mission 3 external payload mounting due to its higher ground clearance.

Conceptual Design phase yielded the following configuration of the aircraft to achieve optimal performance: Conventional monoplane configuration, tricycle landing gear, single tractor propulsion system, high wing and a conventional tail. An aggressive integrated configuration, sizing, propulsion and aerodynamic program is used to minimize the aircraft's RAC while still making it mission-ready.



Figure 3.5: Conceptual Sketch

## 4 PRELIMINARY DESIGN

Preliminary design relies on the conclusions drawn from the conceptual design, and provides a crucial start point for the final design. This phase emphasizes on various trade off studies and optimization processes, governed by mission models and equations. Iterations ensure maximization of Overall Score.

### 4.1 Design and Analysis Methodology

The goal of the Preliminary Design was to arrive at a high-scoring design. An optimization program called the V\_Design, was written by the team in MATLAB®, which uses Genetic Algorithm (GA) to optimize the various parameters of the plane and maximize the Overall Score. GA is a search heuristic that mimics the process of natural selection. This heuristic is routinely used to generate useful solutions to optimization and search problems.[7]

Every parameter that is to be optimized is referred to as a design variable. A single script file calls the GA function, which optimizes a function named F\_Score. Once the GA initializes the design variables, the F\_Score function selectively distributes it into three mission modules simultaneously. Mission modules consist of weight build-up, drag, stability and propulsion modules. Based on the results of these modules, constraint model and mission model, the feasibility of the design is validated. A modified Total Mission Score function served as the cost function for the optimization algorithm. Figure 4.1 depicts the flow of the entire program.

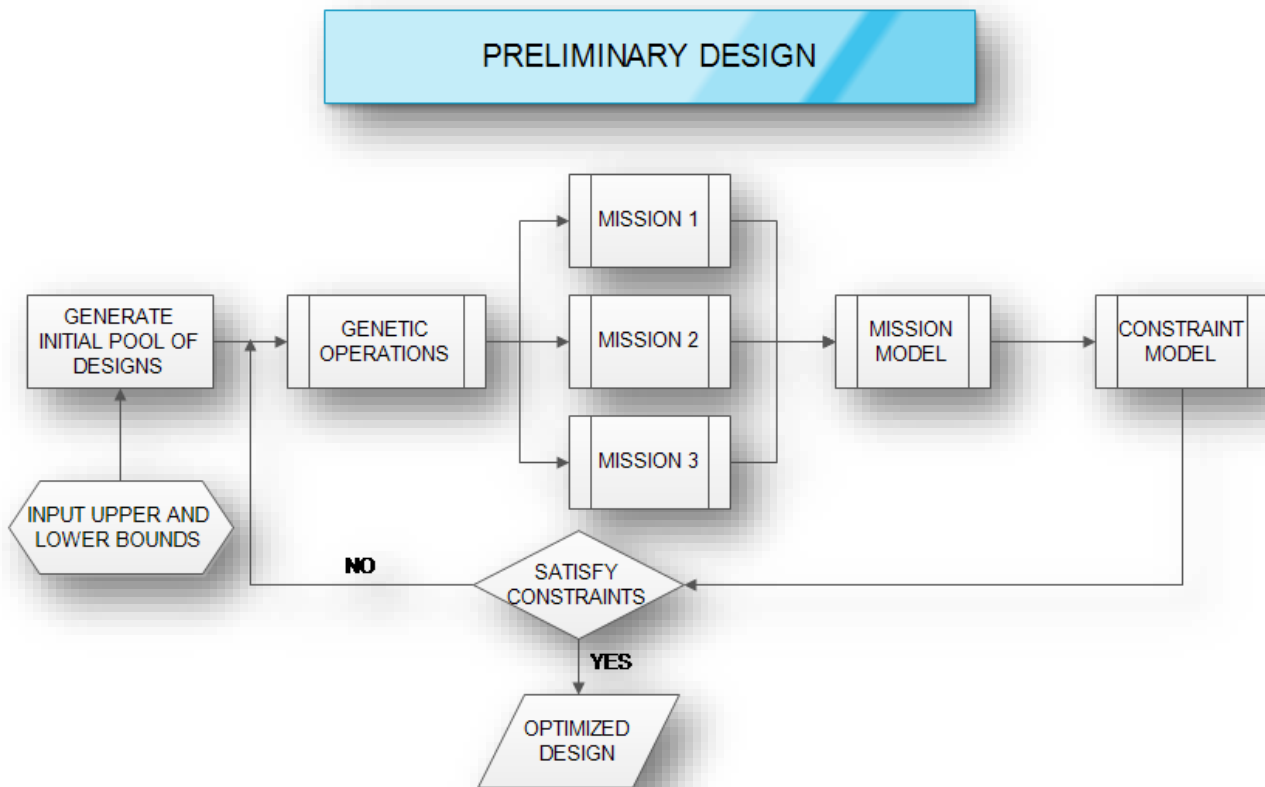


Figure 4.1: Preliminary Design Flowchart

#### 4.1.1 Features

##### Design variables

The main script file contains the lower and upper bound vector for all the design variables. The bounds for most of the parameters were selected based on the team's past experience in designing R/C aircrafts, while the remaining parameters were dictated by the mission requirements such as high flight speed for Mission 1, payload dimensions, its weight and wing area for Mission 2 and ball-drop mechanism placement for Mission 3.

##### Weight build-up

Weight build-up was estimated using the documentation of material densities, manufacturing history and manufacturer specified weight for all the electronic components. As and when manufacturing methods were refined, new data obtained were incorporated into the code.

##### Drag build-up

Drag build-up is estimated using drag estimates from Introduction to Flight by J D Anderson. The parasite drag coefficient of the entire plane is calculated via a drag build up that includes each component of the plane, using relevant formulae. The induced drag is obtained from Athena Vortex Lattice (AVL).

## Stability

This module calculates static margin, all the stability derivatives and eigenvectors for all three mission configurations. However, the eigenvectors just give a general trend of change in dynamic stability for various initialized designs. Hence, to get an accurate picture, AVL and XFLR5 were used.

## Propulsion

Motor-battery-propeller combination is determined by the propulsion model. This model takes in battery voltage, airspeed, propeller and motor specifications as inputs. V\_Design initializes these parameters at the start of the program. This model incorporates propeller performance data and motor characteristic graphs to calculate thrust values, current draw and pitch speeds for different combinations.

Results which are obtained after the evaluation of these modules are fed to mission model and constraints model. Mission Model simulates aircraft performance on the flight course. Constraint Model along with a modified cost function, checks for the design feasibility in all aspects. These models are further elaborated in the subsequent section.

## 4.2 Mission, Constraint and TMS Models

### 4.2.1 Mission Model

The mission model serves as a basic criterion for selecting feasible designs from the initialized lot. With the available weight, drag and propulsion estimate for each aircraft, the model estimates the Total Mission Score by simulating all the three flight missions along different parts of the competition course as shown in the figure.

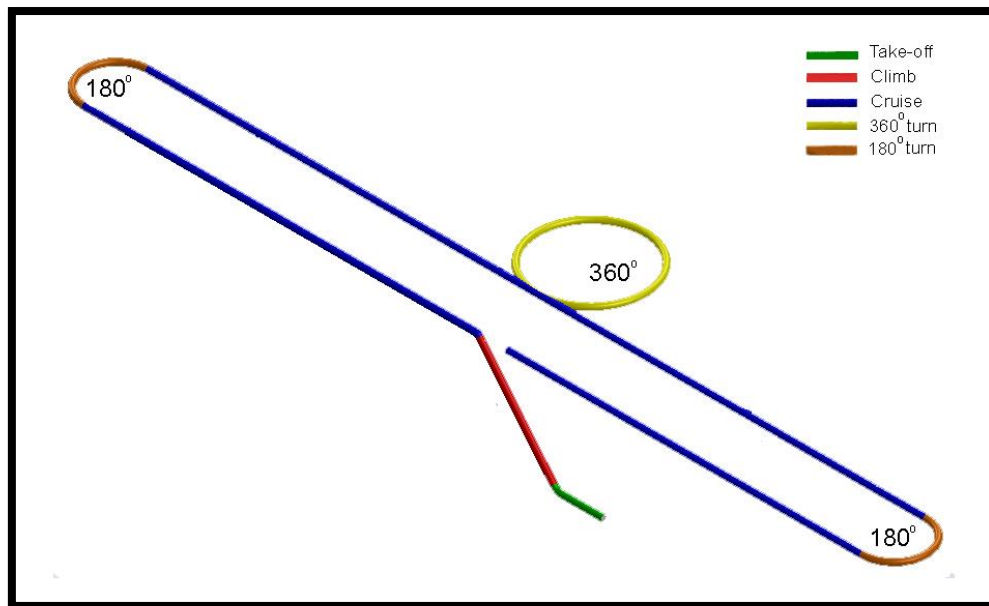


Figure 4.2: Flight Course

1. **Takeoff:** Aircraft starts from rest and starts accelerating at full throttle. Flaps were deployed to increase  $C_{Lmax}$ . Wing area was the most critical parameter to satisfy takeoff distance criteria of 60-ft, especially in mission 2.
2. **Climb:** This maneuver is based on the excess power available and the aircraft was assumed to climb to 75 feet.
3. **Turn:** Aircraft is assumed to enter the turn at a reduced speed and execute the same at a constant speed. The turn radius was calculated assuming a constant load factor. Any drop in altitude of the aircraft that may occur was neglected.

**4. Cruise:** Steady unaccelerated flight with equal thrust and drag was assumed. The aircraft was simulated to fly at full throttle in this maneuver for Mission 1 and 2. However, for Mission 3, less than full throttle setting was assumed to maximize endurance of the battery.

#### 4.2.2 Constraint model

The mission model, while simulating the aircraft along the flight course, doesn't consider the plane's stability parameters and safe operating ranges. To account for all these factors, a vector belonging to the constraint space [g(x)] was created.

In this vector, the value of each element is dependent on the constraint type of the parameter in question. Each parameter belonged to one of three intervals viz., left open-ended (-inf, a], two-side bounded [m, n], right open-ended [p, inf). Based on the interval type to which they belonged, different kinds of equations were used. General form of those equations is shown in table 4.1.

Table 4.1: General form of Constraint Equations

UPPER LIMIT	LOWER LIMIT
$g \leq g_u$ $\Rightarrow \frac{g}{g_u} - 1 \leq 0$	$g \geq g_L$ $\Rightarrow 1 - \frac{g}{g_L} \leq 0$

#### 4.2.2 Total Mission Score Model (F\_Score)

The cost function is critical to obtain optimized design. The scores generated based on Total Mission Score equation [f(x)] alone cannot be used to evaluate the generated design, as it doesn't consider the constraint vector. To account for this, a pseudo-objective function (phi) was created. This function summed up the generated scores and the constraint vector elements.

$$phi(x) = f(x) + \sum_{i=1}^n g_i(x) \quad (Eq.4.1)$$

During optimization, ideally every constraint element has to be equal to zero. However, it was found out otherwise. To address this problem, number of generations was increased from recommended value of 100 to 1000.



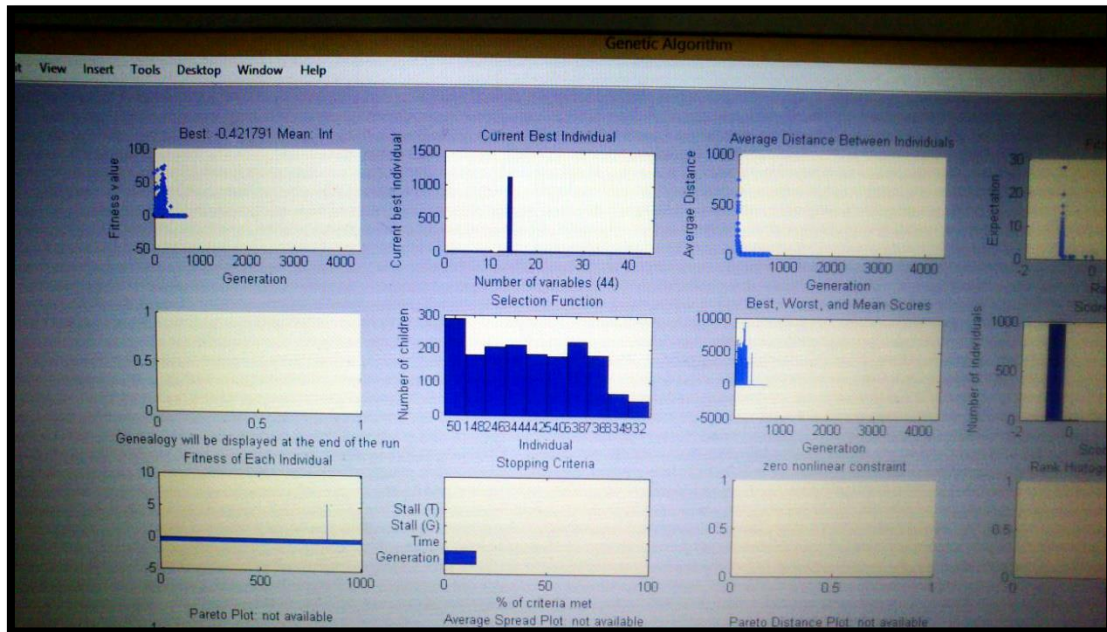


Figure 4.3: Converged Design Point

The value of Total Mission Score / RAC obtained in the code was  $-0.4217$ . Other parameters relating to the score are discussed in section 4.6.

#### 4.2.3 Assumptions and Uncertainties:

- To calculate a Total Mission Score for generated designs, best aircraft in the competition is assumed to complete 9 laps in Mission 1, complete 3 laps within 100 seconds in Mission 2 and carry and drop 8 balls in Mission 3.
- No headwind or crosswind was assumed during the simulation of the missions. While presence of a moderate headwind would contribute positively towards aircraft performance, crosswind would pose a challenge in controlling the aircraft.
- The mission model estimated motor and propeller performance on empirical equations and data. Manufacturer stated battery capacities and voltages were used in the model. The current drawn was assumed to be constant throughout the flight (except at takeoff).

### 4.3 Design and sizing trades

#### 4.3.1 Selection of number of balls for mission 3

The number of Champro balls to be carried is dictated by the code itself. Linking this selection to other design parameters is crucial for its optimization.

As described in section 3.4.5, the balls were to be placed under the fuselage. However, they cannot be placed for the entire length of the aircraft for two reasons.

Firstly, the axis of the mechanism is along one plane. But the aircraft has a boom configuration and would not permit this placement. Secondly, the balls have to be dropped one per lap flown. If this placement is employed, there would be large variations in C.G, due to large moment arm of balls placed at the ends. The above considerations are difficult to implement in the code.

To counter this problem, the aircraft was divided into three sections along the length viz., firewall to leading edge, aircraft under the wing and the empennage. The mechanism was decided to be placed under sections one and two, which comprise the fuselage of the aircraft. Hence, the selection was to be linked with the chord of the wing, overall C.G. position and locations of mission 2 payload and battery, which dictate the dimensions of the fuselage. Result obtained from the program was to carry four balls, and mechanism was to be placed under the fuselage only.

### 4.3.2 Airfoil selection

The airfoil selection process involves the evaluation of several airfoils using a 2D flow simulation software for testing and making comparisons of these results, as well as other characteristics.

Airfoils were chosen from the UIUC airfoil database[4] for analysis. Reynolds Number has a significant impact on the effectiveness of an airfoil. Relatively thick airfoils provide structural viability and prevent flow separation. These two parameters led the team to shortlist 24 airfoils which would perform satisfactorily. The mission requirements further implicitly defined more parameters, which served as criteria for selecting the best airfoil. The parameters were – High lift coefficient to satisfy the take-off distance criteria, low parasite drag to attain high cruise velocity and to reduce power requirement, small pitching moment to minimize trim drag, and a high stall angle.

The shortlisted airfoils were analyzed using XFLR-5, at the estimated Reynolds number of 4, 00,000. The flow analysis tool provided valid results at this regime. The results were subjected to FOM analysis in batches. The parameters were weighed on the basis of their importance. The mission requirements dictated the ranking of these parameters. In descending order of importance –  $C_{Lmax}$ ,  $C_L/C_D$ ,  $C_{Dmin}$ ,  $\alpha$  at  $C_{Lmax}$ ,  $C_m$  v/s  $\alpha$

This led the team to arrive at the 4 best performing airfoils as shown in figure 4.4.

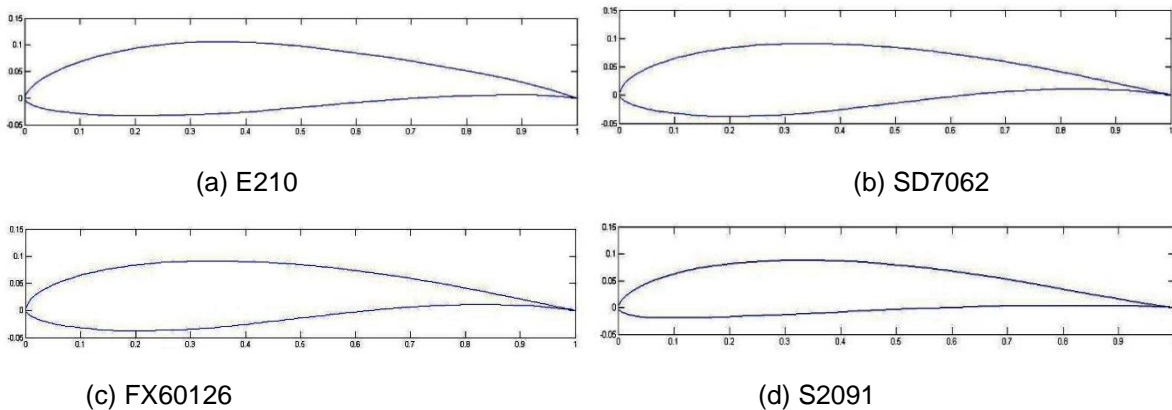

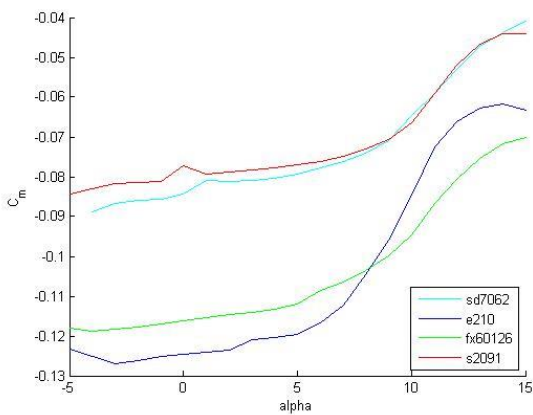


Figure 4.4: Best Performing Airfoils

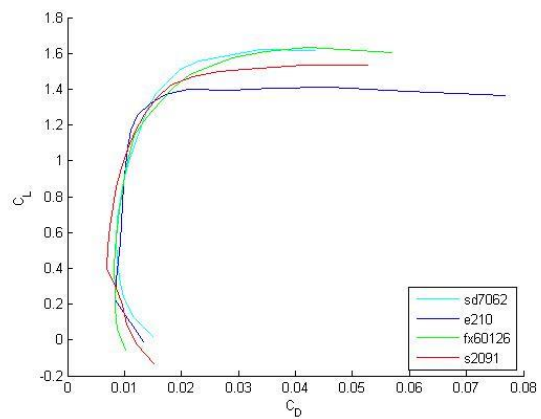
The following table presents the comparison among the best performing airfoils.

Table 4.2: Airfoil Decision Matrix

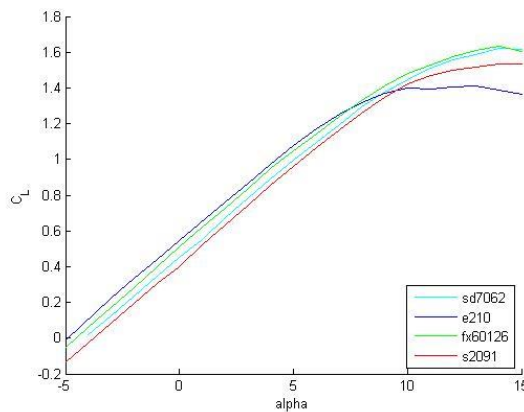
		e210	sd7062	fx60126	s2091
		Norm Rating	Norm Rating	Norm Rating	Norm Rating
Requirements	Norm Weighting				
$C_{Lmax}$	0.28	1	4	4	3
$C_L/C_D$	0.28	4	2	1	3
$C_{Dmin}$	0.20	1	2	3	4
alpha @ $C_{Lmax}$	0.12	1	4	4	3
$C_m$ vs alpha	0.12	1	4	2	4
<b>Grand Total</b>		<b>1.84</b>	<b>3.04</b>	<b>2.72</b>	<b>3.32</b>



(a)  $C_m$ -alpha Graph



(b)  $C_L$ - $C_D$  Graph



(c)  $C_L$ -alpha Graph

Figure 4.5 Lift, Drag and Pitching Moment Curves for the final 4 airfoils

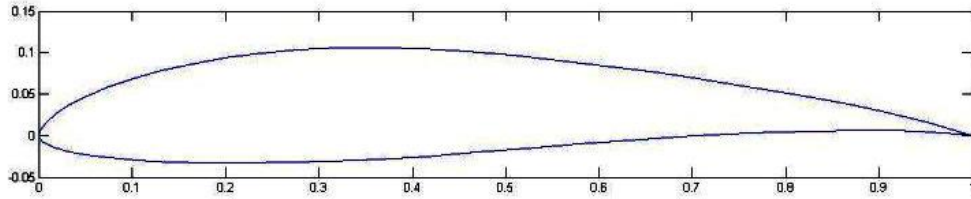


Figure 4.6: S2091

The airfoil yielding optimal performance over the three missions is S2091. It has a high  $C_{Lmax}$  value, high lift to drag ratio, and low  $C_D$  for the design. Additionally, the low pitching moment and desired  $C_m$  curves are beneficial.

Table 4.3: Characteristics of S2091

CHARACTERISTIC	VALUE
$C_{Lmax}$	1.54
Thickness	10.11%
Camber	3.91%
alpha @ $C_{Lmax}$	14°

#### 4.4 Propulsion model

To determine each component of the propulsion system, the output of the propulsion model was meticulously linked with the design variables. For instance, thrust obtained by a certain combination heavily influenced the take-off distance. This was crucial for Mission 2, as the aircraft had to take-off within 60ft while carrying heavy payload. The propulsion model made use of an electric motor model [6] and APC propeller performance [5] data to estimate static thrust, current drawn during take-off, and average power consumed during the flight. Various motors and gear ratios were considered.

The objective of the electric motor model was to generate characteristic graphs which define a brushless motor. Here, the model uses only two graphs – Torque v/s Angular velocity (Fig 4.7 a) and Efficiency v/s Angular velocity (Fig 4.7 b)

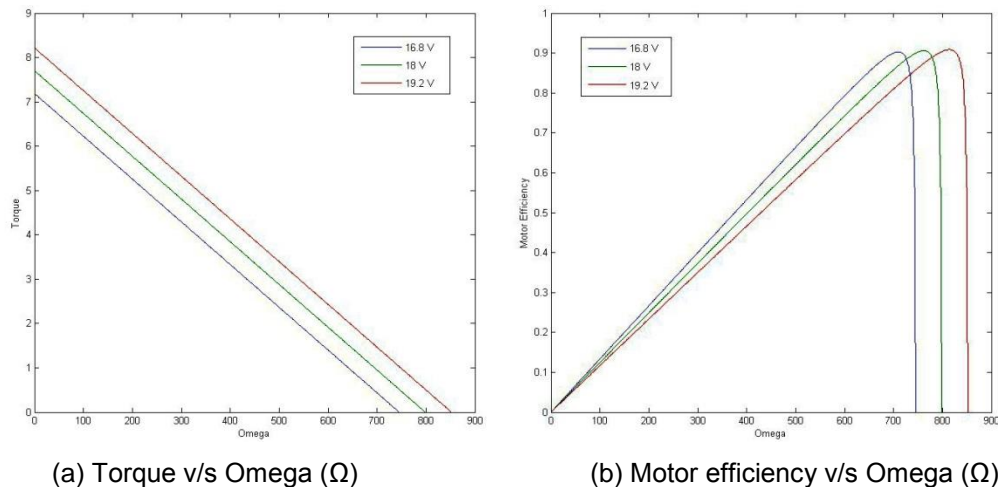


Figure 4.7: Characteristics Graphs of a Motor

It is evident from graphs that the curves are dependent on the input voltage to the motor. Hence, during the optimization process, graphs are generated for that input voltage, which was initialized by the program. These graphs serve as the basis for the selection of a propeller. Generally, a propeller is characterized by the thrust and power coefficients, which depend primarily on the advance ratio and RPM at which it is rotated. Once the propeller geometry is initialized by the program, the  $C_t$ ,  $C_p$  and efficiency curves generated. By fixing free stream velocity for each mission, advance ratio depends only on rpm. Following graphs shows the variation of these parameters with respect to rpm.

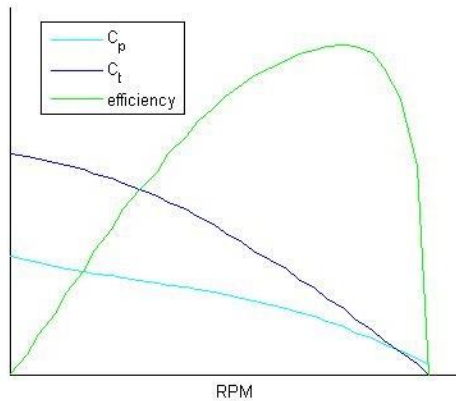


Figure 4.8: Variation of  $C_t$ ,  $C_p$  and efficiency with RPM

The equilibrium operating RPM of the motor/prop combination occurs when the torques are equal.

$$Q_m(\Omega, V) = Q(\Omega, v) \text{ (Eq. 4.2)}$$

This is graphically shown in the figure(number), where the torque matching condition is applied to first determine the motor angular velocity ( $\Omega$ ). All the other propeller and motor parameters can then be determined from their respective characteristic curves. The vertical dashed line represents the operating angular velocity.

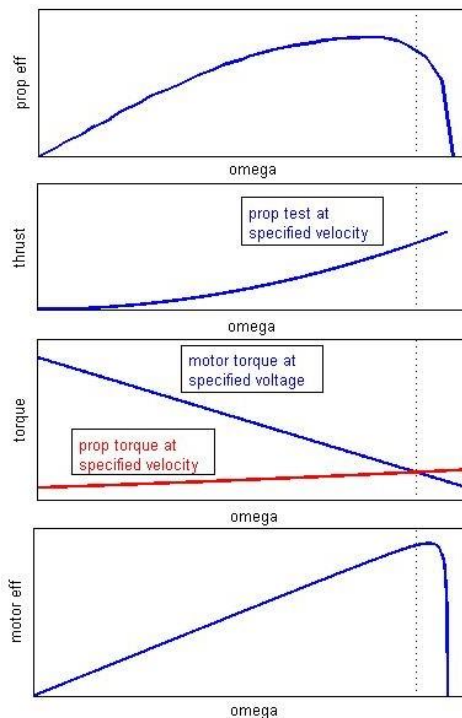


Figure 4.9: Propeller and Motor Parameters obtained from a specified flight speed  $v$  and a specified motor voltage  $V$ . Many battery-motor-propeller-gearbox combinations were iterated by the program to arrive at the optimum design.

Table 4.4: Optimum Propulsion Combination

OPTIMUM PROPULSION COMBINATION		
<b>Battery</b>		15-cell Elite 2000 AA
<b>Motor</b>		Electrifly GPMG 5225
<b>Kv Rating (rpm/V)</b>		1530
<b>Gear Ratio</b>		3.6:1
<b>Propellers</b>	<b>Mission 1</b>	13 x 10
	<b>Mission 2</b>	14 x 8
	<b>Mission 3</b>	13 x 6.5

Various assumptions were made in the model, to reduce the complexity of the iteration. For example, the battery voltage was assumed to be constant and equal to 1.2V per cell. To account for this approximation, the propulsion combination was extensively tested by the team, results of which are discussed in the later sections.

#### 4.5 Lift, Drag and Stability characteristics:

XLFR5 provides lift and drag estimates of the aircraft. Figure 4.10 plots aerodynamic efficiency (L/D) versus aircraft lift coefficient ( $C_L$ ).

Mission 1 and Mission 2 were to be flown at full throttle, since speed was an important factor in scoring. Accordingly, Mission 1 had low cruise  $C_L$  and operated at low L/D values, whereas, mission 2 had comparatively higher  $C_L$  values, due to higher weight and operated near  $L/D_{max}$ . Mission 3 was expected to be flown at approximately 70% throttle to get accustomed to dynamic C.G. position of the aircraft.

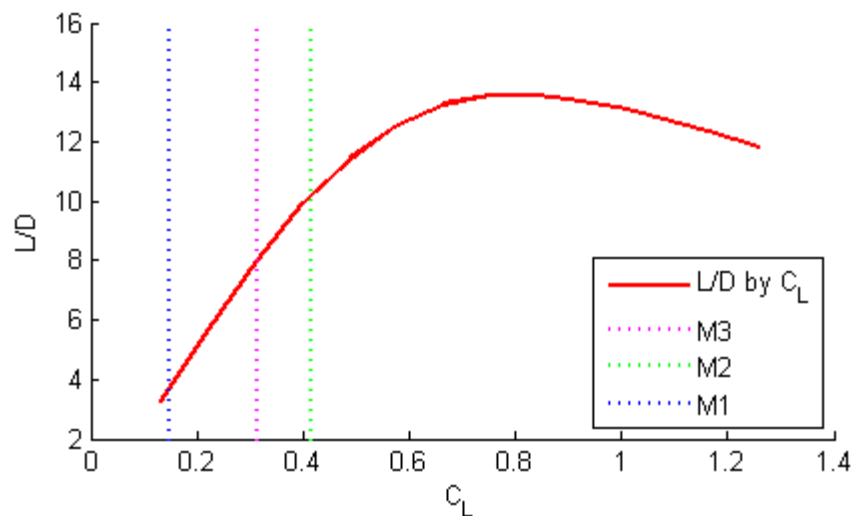


Figure 4.10: L/D vs.  $C_L$  for different cruise conditions

#### 4.5.1 Drag estimation and Build up

Initial drag estimates for the aircraft was calculated after selection of the airfoil and geometric dimensions. AVL was used to estimate the induced drag on the wing and tail surfaces. The parasite drag ( $C_{D0}$ ) build up consisted of estimating the viscous drag on the wings, tails, fuselage, joints, etc. using the drag estimates from Introduction to Flight by J D Anderson [2]. These two drag components were combined for the different missions and shown in Pi chart.

##### Parasite Drag Model

Since the flow is within the low Reynolds number range, a few factors were considered negligible. Such factors include the shock-induced, wave drag, and scrubbing drag. This method estimates the subsonic parasite drag of each component of the aircraft using a flat-plate skin-friction drag analysis.

$$C_f = \frac{0.074}{Re^{0.2}} \quad (Eq. 4.3)$$

This estimation technique implements the flat-plate skin friction analysis, where the skin friction coefficient ( $C_f$ ) depends on the local Reynolds number ( $Re$ ). However, this parasite drag build-up considered the flow to be fully turbulent. This was believed to be a valid assumption considering the imperfect nature of manufacturing techniques and the effect of protrusions, such as linkages, control horns, and control surface gaps.

##### Induced Drag Model

In order to accurately determine the induced drag of the aircraft, AVL was used [11]. It is a standard vortex lattice code that uses horseshoe vortices to determine the inviscid flow of the wing and tail surfaces. The plane model was fed into the program, and the induced drag of the entire model could be estimated.

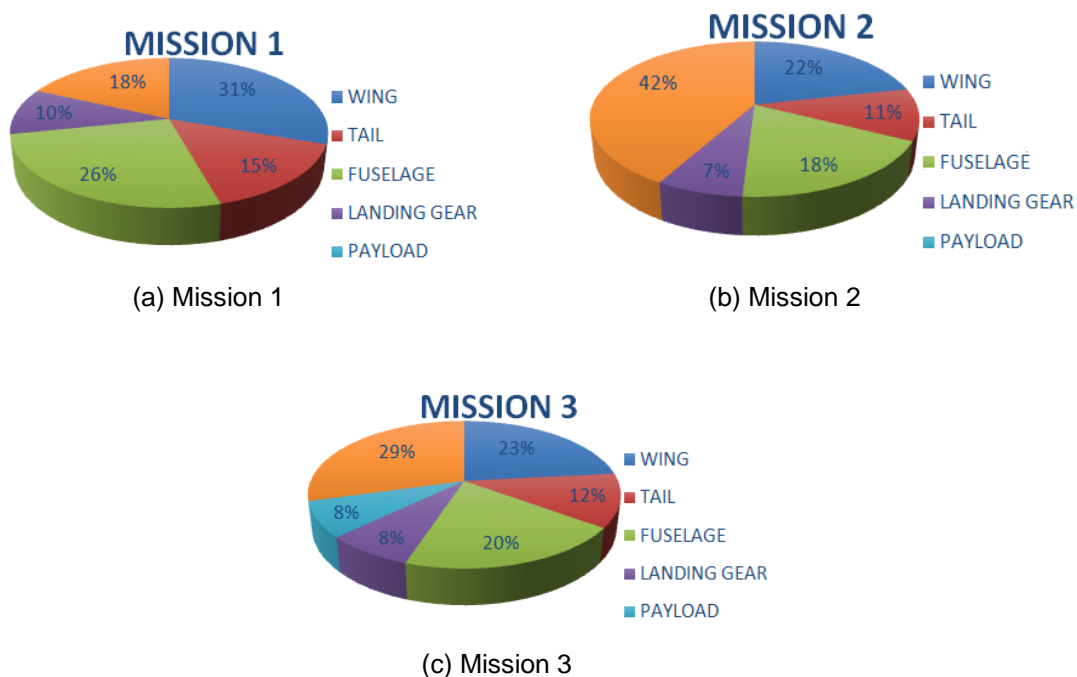


Figure 4.11: Mission-wise Drag Build-up

Table 4.5: Drag breakdown

	MISSION 1	MISSION 2	MISSION 3
<b>WING</b>	0.01177	0.01177	0.01177
<b>TAIL</b>	0.00592	0.00592	0.00592
<b>FUSELAGE</b>	0.01013	0.01013	0.01013
<b>LANDING GEAR</b>	0.00393	0.00393	0.00393
<b>EXTERNAL PAYLOAD</b>	NA	NA	0.00798
<b>INDUCED DRAG</b>	NA	0.02282	0.01481

#### 4.5.2 Stability and control

The aircraft was designed without a rudder which would discount the use of one servo and increase the score by around 20%. So, the ailerons were sized such that the aircraft was more responsive to the deflections even during considerable crosswinds. The controllability of the aircraft in this regard was assessed in the test flights.

Various stability derivatives were calculated to give an idea about the aircraft's stability. It is seen that the derivatives such as  $C_{l\beta}$ ,  $C_{m\alpha}$ ,  $C_{mq}$  are negative and  $C_{n\beta}$  is positive, which corroborates the stability of the aircraft.

Table 4.6: Stability derivatives

COEFF.	VALUE	COEFF.	VALUE	COEFF.	VALUE
$C_{Lq}$	8.6061	$C_{mq}$	-12.0320	$C_{l\delta e}$	0.0144
$C_{L\alpha}$	5.1130	$C_{m\alpha}$	-0.9640	$C_{m\delta e}$	-0.0328
$C_{yr}$	0.1224	$C_{lr}$	0.1120	$C_{nr}$	-0.0411
$C_{y\beta}$	-0.1422	$C_{l\beta}$	-0.0151	$C_{n\beta}$	0.0511
$C_{yp}$	0.0020	$C_{lp}$	-0.5182	$C_{np}$	-0.0323
$C_{y\delta a}$	-0.0005	$C_{l\delta a}$	0.0028	$C_{n\delta a}$	-0.0001

Also, dynamic stability analysis was carried out in AVL. Figure 4.12 shows a root-locus plot for five modes of stability for aircraft loaded with Mission 2 payload. It was seen that the aircraft was unstable in spiral mode. The aircraft would be pushed into a spiral path if it were to be perturbed by a large crosswind. However, it was found that it can be corrected easily by the pilot.

But Mission 3 involves dropping payload (Champro Balls) during each lap. The C.G position of the aircraft varies along the length of the aircraft. This leads to change in equilibrium angle of attack. Hence, dynamic stability analysis was done for C.G position at different instances to confirm its stability.



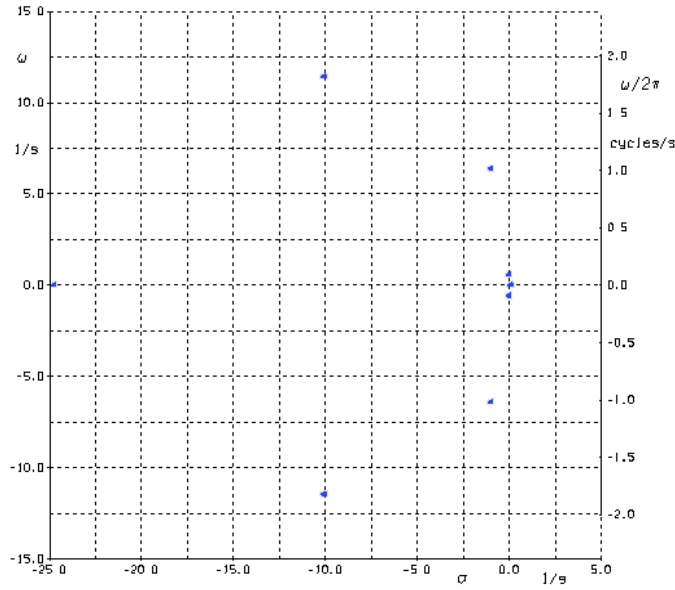


Figure 4.12: Root-locus plot

## 4.6 Predicted Mission Performance

Table 4.7: Preliminary Aircraft Predicted Performance

PERFORMANCE PARAMETER	MISSION 1	MISSION 2	MISSION 3
Cruise Speed (ft/s)	75.7	65.6	55.7
#Laps	6	NA	NA
Time taken (s)	NA	127	NA
#Balls	NA	NA	4
TOGW (lbs)	3.52	8.37	4.12
Score	1.33	3.15	3.00

Table 4.8: Preliminary Aircraft Predicted Scoring

SCORING	
#Servos	5
Max Empty Weight (lbs)	3.52
Total Mission Score	7.48
RAC	17.6
Total Mission Score/RAC	0.42

Table 4.7 gives a brief idea of the performance of the aircraft in all the missions. The mission one and two scores are expected to be competitive. However, there is a factor of uncertainty regarding mission three due to the possibility of different designs of dropping mechanisms. This makes it difficult to predict the mission 3 score. Also, the team intends to conduct extensive testing to reduce the number of servos, which has a significant impact on the Overall Competition Score.

## 5 DETAILED DESIGN

The dimensional and performance parameters, structural characteristics and sub-systems design along with selection and integration of the final aircraft design are documented in this section of the report. From sensitivity analysis, it was found that RAC and Ground Score were the most influential parameters affecting the Overall Score. The process of detailed design was carried out by assigning the highest priority to these factors along with feasibility and ease of manufacture.

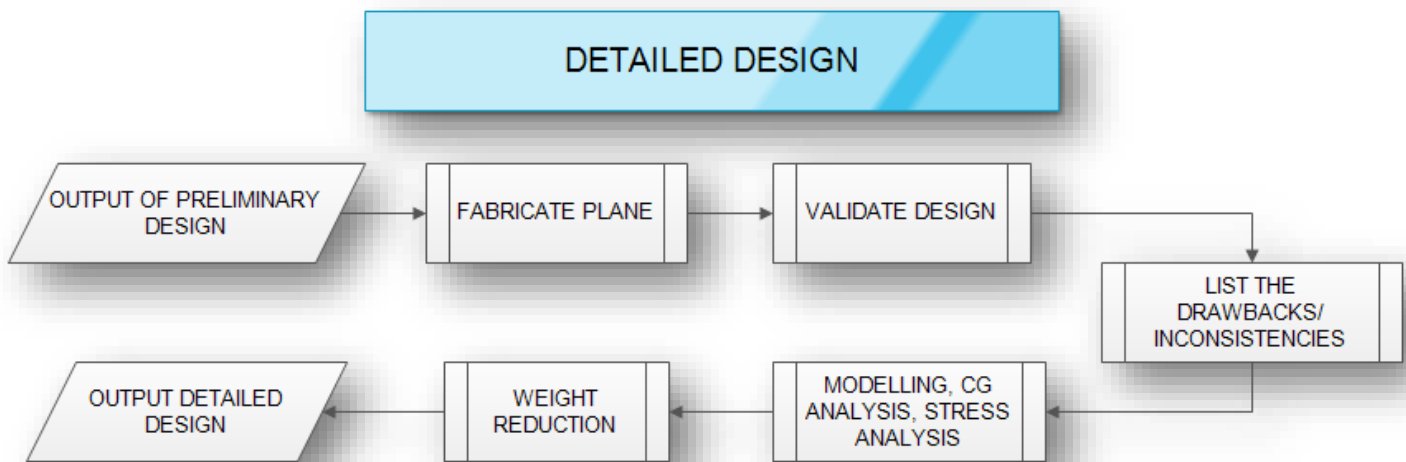


Figure 5.1: Detailed Design Flowchart

### 5.1 Dimensional Parameters

Table 5.1 shows the major characteristic parameters of the plane.

Table 5.1: VYOMA Characteristic Parameters

Wing		Horizontal Stabilizer		Vertical Stabilizer	
Airfoil	s2091	Airfoil	sd7037	Root chord (in)	6.7
Span (in)	67.71	Span (in)	20.47	tip chord (in)	1.57
Chord (in)	9.44	Chord (in)	8.66	Area (in <sup>2</sup> )	30.92
Area (in <sup>2</sup> )	639.18	Area (in <sup>2</sup> )	177.32	height (in)	7.48
Aspect ratio	7.11	Incidence angle	-4 <sup>0</sup>	Airfoil	Flat plate
Incidence angle	2 <sup>0</sup>	Battery		Motor	
Static margin (%age)	19	Model	Elite 2000mah	Kv (rpm/V)	1530
		Cell Voltage (V)	1.2	Power (W)	425 (continuous)
		Cell Count	15	Weight (g)	200
		Pack Voltage (V)	18	Gear Ratio	3.6:1
		Pack Weight (lbs)	1	I <sub>0</sub> (A)	0.83
Propellers		Controls		Fuselage	
M1	13x10	ESC	Power HD 50 A	Length (in)	25.82
M2	14x8	TX RX	FlySky	Width (in)	7.08
M3	13x6.5	Servo	Emax	Height (in)	6.96

## 5.2 Structural Capabilities and Characteristics

It is vital to ensure that the aircraft is capable of withstanding loads experienced during each of the three missions. The plane weighs around 4 kg when loaded with Mission 2 Payload. The wing was designed to carry the entire weight of the plane and also withstand the high G-forces experienced during turns.

Based on the dimensions obtained in the preliminary design, a prototype was built and tested for validation of design. The aircraft was modelled in SolidWorks®, and analyzed for stresses using the built-in Finite Element Analysis (FEA) module. This provides information on the stress distribution over the entire aircraft. This indicated the regions which had a tendency to fail when loaded, using which structural reinforcements were provided. Also, it facilitated weight reduction at non-loaded regions.

The goal of this phase is to arrive at a design whose structure must be robust and at the same time lightweight. Different composites like glass fiber and carbon fiber were experimented to meet this criterion. At areas where it was necessary to maintain just the profile, balsa wood with lightening holes was employed and at areas where loading was of importance, carbon fiber reinforced balsa wood was used. In an effort to maximize the Ground Score, adequate emphasis was laid on the simplicity of the payload mounting mechanism.

## 5.3 Systems and Subsystems Design

### 5.3.1 Wing

The main wing was designed to provide the optimal wing loading required to perform all missions. It is composed of balsa wood and carbon rods. The wing, being the most difficult component of the aircraft to build, was fabricated in two halves to facilitate its transportation and to avoid last minute complications. The ribs, which form the skeleton of the wing, were laser cut to get the required airfoil profile. Initially the ribs were cut from a 3.5 mm balsa board. During the finalization of the aircraft structure, the team realized that 2.5 mm balsa fell well within the factor of safety, and hence provided a window for weight reduction. A 14mm OD and 12mm ID carbon tube was used as the main spar. Lightening holes were cut in the ribs and flaperons to reduce weight. 1mm Balsa sheets were used to cover the leading edge in order to impart torsional strength to the wing.

Opting for fabrication as two half-wings posed another challenge which was the joining process of the two halves. Due to the discontinuity, there is a high probability of fracture occurring at the joints. In order to address this, the team came up with the solution as shown in figure 5.2.

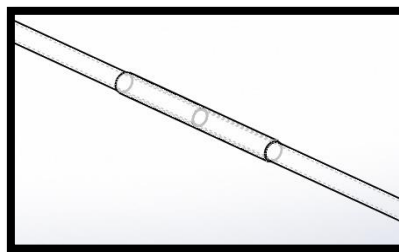


Figure 5.2: Wing joint- Wire frame model

A 16mm OD and 14mm ID carbon tube forms the outer covering at the junction. This joining process proved to be a viable option as it effectively distributes the load on to fuse hence preventing structural failure. The wing skeleton is covered in Microlite®. Finally, a 25% reduction in weight with respect to the first prototype was achieved.

### 5.3.2 Fuselage

The fuselage is composed of balsa wood. It was designed as a set of jigsaw pieces, thus making it easier to fabricate and transport. It was designed to accommodate and effectively secure mission 2 and mission 3 payloads. Further it is shaped aerodynamically to minimize parasite drag.

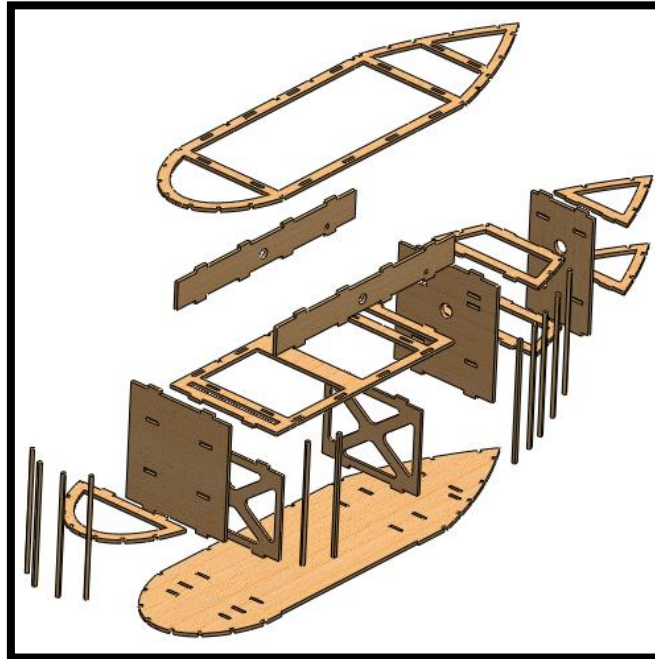


Figure 5.3: Exploded View of Fuselage

The semi-monocoque type of structure was selected in order to achieve the required shape. Stringers were employed for torsional rigidity. Carbon fiber stringers were employed only at the payload bay, to withstand the loads exerted by the payload. The Payload bay was positioned to make the payload C.G coincide with the aircraft C.G, thus avoiding complications during the process of balancing the C.G for different missions. The firewall was reinforced with carbon fiber so as to withstand the thrust of the motor. Holes were cut out in the bulk head to fix the boom at the calculated angle of -4 degrees with respect to horizontal. The battery pack, receivers, speed controller and servos were positioned accurately to maintain the C.G and increase the ease of accessibility.

### 5.3.3 Empennage

The conventional tail configuration is easier to mount on a boom. The boom structure was chosen as it was lighter and stronger than the conventional truss structure. A carbon fiber rod was chosen because of its high strength and reliability. Both horizontal and vertical stabilizers were mounted onto the boom using 2mm carbon rods that run through them.

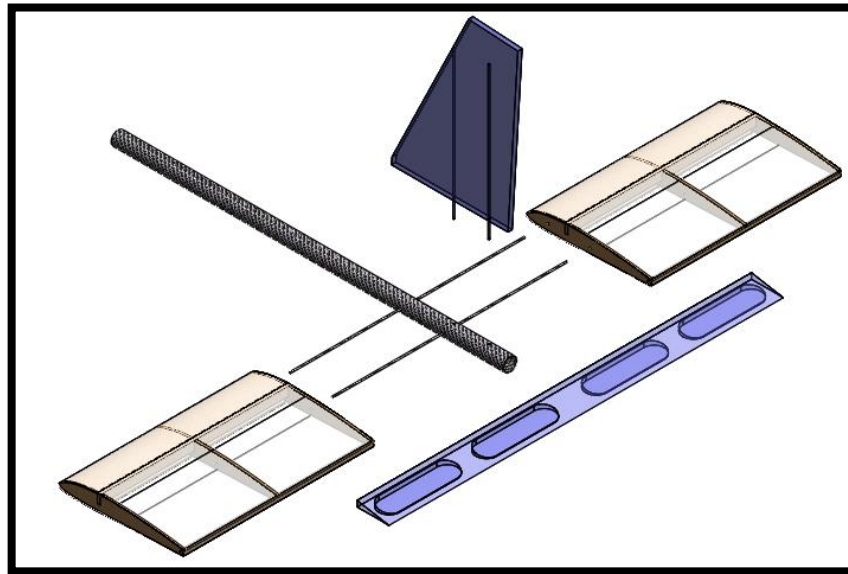


Figure 5.4: Exploded View of Empennage

### 5.3.4 Electronic Components Selection

#### Servo selection

The most crucial parameter to be considered for selecting a servo is torque requirement. Hinge moment coefficients were calculated using AVL for maximum velocity and the corresponding torque requirements were calculated. Table 5.2 shows the calculated hinge moments and corresponding torque requirements. The flaperon and elevator servos were selected based on the torque requirements and ease of availability. Table 5.3 shows the selected servos for flaperon and elevator.

Table 5.2: Hinge moments

CONTROL SURFACE	$C_{hm}$	TORQUE (oz-in)
Flaperon (per servo)	6.395E-03	28.85
Elevator	3.791E-03	17.10

#### ESC Selection

The team selected the Electronic Speed Controller (ESC) based on the maximum current capacity of the motor. The ESC possesses a Battery Eliminator Circuit (BEC) which is capable of powering the receiver directly from the main battery pack. However, this would result in violation of the General Aircraft Requirements. In order to adhere to the requirements, only the signal wire was taken from the ESC and the receiver was powered using a separate battery.

Table 5.3: The chosen propulsion and control systems for the final design

COMPONENT	MANUFACTURER	MODEL
Flaperon Servo	Emax	ES08MD 12g (0.42 oz)
Elevator Servo	Emax	ES08MD 12g (0.42 oz)
Motor	Electrifly	Ammo inrunner GPMG 5225
Main Battery	Elite	2000 mAh AA
ESC	Power HD	50A
Servo for dropping mechanism	Turnigy	TG9e 9g (0.31 oz)
Receiver	Flysky	I6
Transmitter	Flysky	I6

### 5.3.5 Landing Gear

A tricycle configuration was selected for its superior ground handling, ease of manufacture and the ability to accommodate external payload mechanism. Since RAC has a large impact on the Overall Score, servos have to limited to a minimum number. Thus the nose landing gear was not provided with any servo for steering.

The nose landing gear was manufactured specifically to ensure that the aircraft maintains a straight path for a minimum distance of 60 feet. The main landing gear was fabricated out of carbon fiber. The shape of the landing gear was designed to flex and bend, which in turn would avoid transmission of impact load to the fuselage. The height of the main landing gear was determined considering the space constraints posed by Mission 3 payload. The nose landing was manufactured using a steel strut. Height of the nose landing gear was decided based on the angle of attack required during take-off. The Landing gear positioning and wheel base were determined based on the general requirements such as takeoff roll and pitching moments [8].

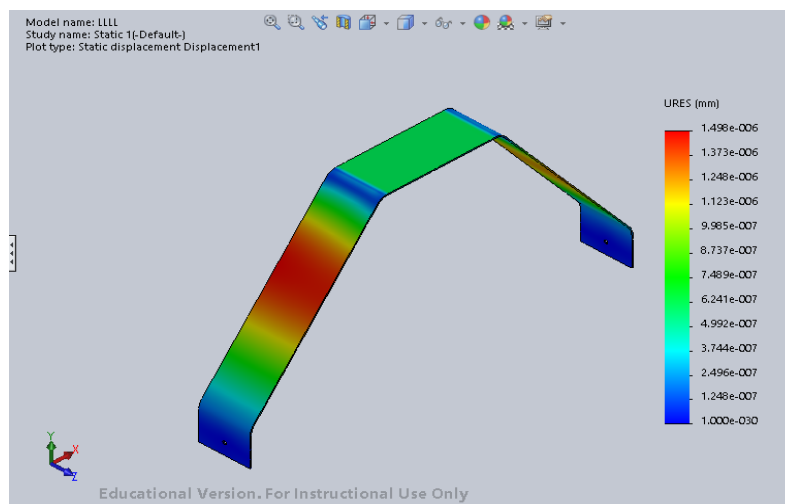


Figure 5.5 Deflection in the main landing gear

The width of the main landing gear was decided based on the results obtained through SolidWorks® FEA. The team arrived at the final dimensions of the landing gear, which could withstand loads up to 16 Kg. This complied with a factor of safety of 4. Figure 5.5 represents the deflection due to stresses in the main landing gear.

### **5.3.6 Payload**

Restraining the payloads is one of the basic requirements of the aircraft. The ground mission demands the loading of Mission 2 payload and Mission 3 payloads and unloading of Mission 2 payload, in the shortest possible time. Thus the securing mechanism had to be simple and robust. The mechanisms and restraints considered for Mission 2 and Mission 3 are further elaborated in the section 5.7.

#### **Mission 2**

The payload bay for mission 2 was integrated in the fuselage design. Foam was used on the sides of the payload bay to constrain the payload. The payload bay was designed to fit the maximum dimensions of the payload, i.e. for outer tolerance limit, along with allowance for the foam. The bay, with the foam, was made to enclose the minimum dimensions of the payload. The foam compresses and secures mission 2 payload with negative and positive tolerances successfully.

The payload door is located below the wing, on the side of the fuselage. It was fitted with neodymium magnets for faster loading time. The size of the neodymium magnets was decided by experimental testing, such that it withstands the entire weight of the payload resting on it.

#### **Mission 3**

The dropping mechanism was constructed keeping the ground score in mind. Maximum number of balls have to be loaded by the time the second mission payload is unloaded. Two balsa rings and three spars make up the basic structure for holding the balls. The dropping mechanism is a C shaped rod pivoted by a servo. This rod ensures that the balls are released one at a time. One of the spars being telescopic allows for loading the balls.

## **5.4 Weights and Balances**

It was necessary to determine the weights and balance of all the components that comprise the aircraft. This would enable the team to determine the CG of the aircraft. The moments were taken about the nose of the aircraft, with +ve X axis being towards the tail, +ve Y axis towards the left wing from Pilot's perspective and +ve Z axis extending upwards from the top of the fuselage.

Table 5.4 shows the weights and balances of the empty aircraft. The empty aircraft weighs just above 1.8Kg. The subsequent tables viz., Table 5.5 and 5.6 give the weights and balances of the aircraft in Mission 2 and Mission 3.

Table 5.4: Weights and Balances

COMPONENT	MASS (oz.)	X (in)	Y (in)	Z (in)
Wing	10.58	11.43	0	-1.08
Boom	1.75	28.55	0	-1.93
Horizontal Stabilizer	2.06	36.72	0	-1.32
Vertical Stabilizer	0.94	37	0	3
Main Landing Gear	2.29	12.65	0	-11.11
Nose Landing Gear	1.34	0.80	-0.52	-10.82
Fuselage	11	12.26	0.16	-3.92
Motor	11.52	1.80	0.02	-3.46
Left Flaperon Servo	0.42	11.76	18.6	-1.07
Right Flaperon Servo	0.42	11.76	-18.6	-1.07
Elevator Servo	0.42	17.41	1.12	-2.6
Dropping Mechanism Servo	0.812	17.08	-2.36	-7.69
ESC	1.58	3.83	-1.76	-1.35
Battery Pack	15.87	9.2	0	-0.98
Receiver Pack	2.11	16.56	0	-1.43
Receiver	1.05	3.70	2.75	-0.5
<b>Total</b>	<b>64.25</b>	<b>10.75</b>	<b>0</b>	<b>-2.60</b>

Table 5.5: Weights and Balances for Mission 2

COMPONENT	MASS (oz.)	X(in)	Y(in)	Z(in)
Empty airplane	64.25	10.75	0	-2.60
Mission 2 payload	80	10.74	0	-4.43
<b>Total</b>	<b>144.25</b>	<b>10.74</b>	<b>0</b>	<b>-3.6</b>

Table 5.6: Weights and Balances for Mission 3

COMPONENT	MASS (oz.)	X(in)	Y(in)	Z(in)
Empty airplane	64.25	10.75	0	-2.60
Mission 3 payload	9.60	11.95	0	-9.12
<b>Total</b>	<b>73.85</b>	<b>10.9</b>	<b>0</b>	<b>-3.45</b>



## 5.5 Flight performance parameters

Table 5.7 represents various parameters that will be helpful in analyzing the flight performance in three flight missions.

Table 5.7: Performance Parameters

PERFORMANCE PARAMETER	M1	M2	M3
Flight Weight (lbs)	4	8.81	4.4
$C_{do}$	0.03175	0.03175	0.03973
Take-off Distance (ft)	12	51	21
Cruise velocity (ft/s)	75.7	65.6	55.7
Stall velocity (ft/s)	22.24	34	23.45
$C_L$ cruise	0.148	0.414	0.314
W/S (lbs/ft <sup>2</sup> )	0.992	2.083	1.141
L/D cruise	4.66	13.0393	7.903

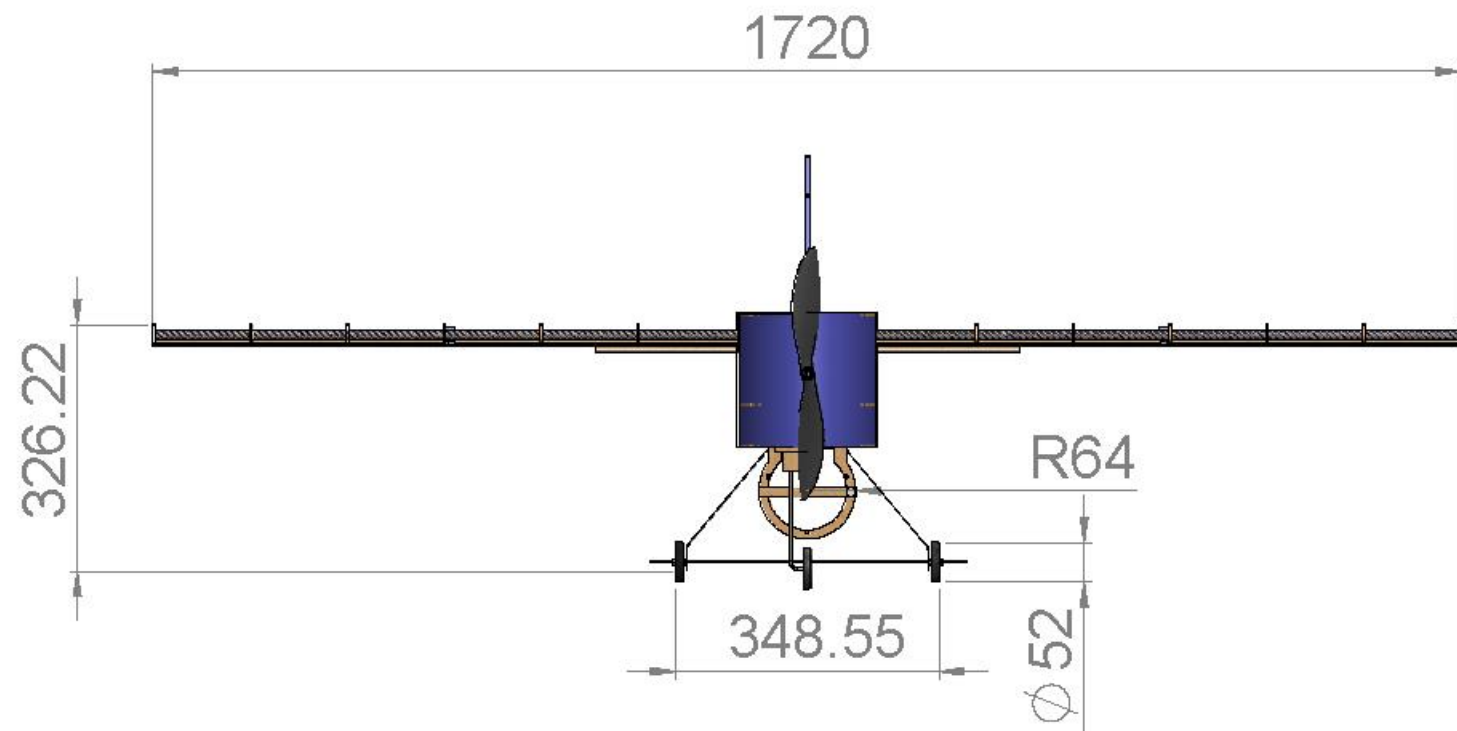
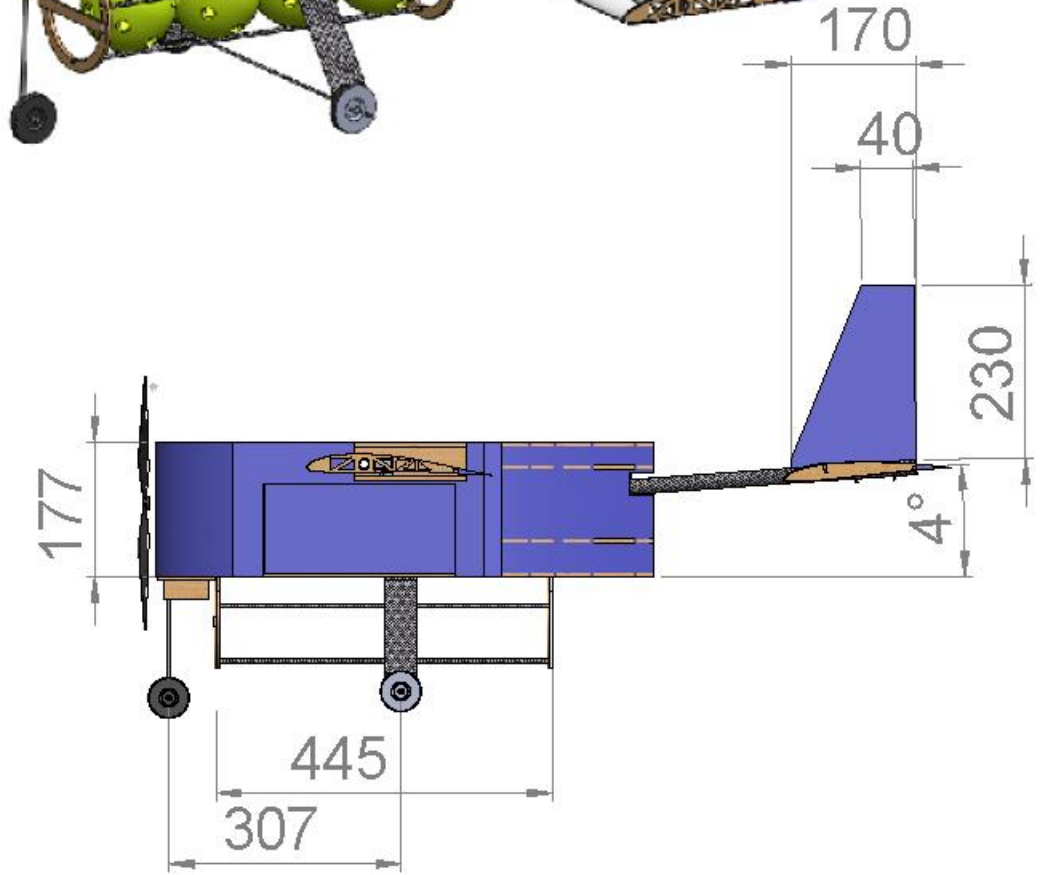
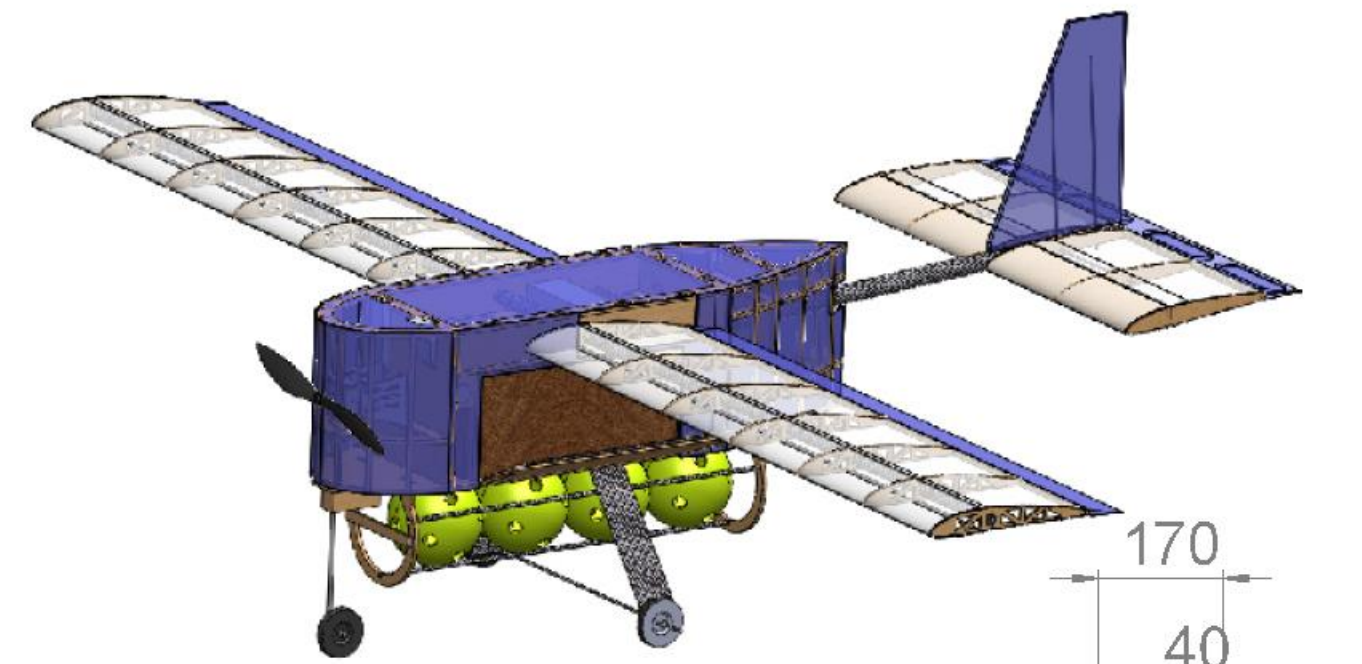
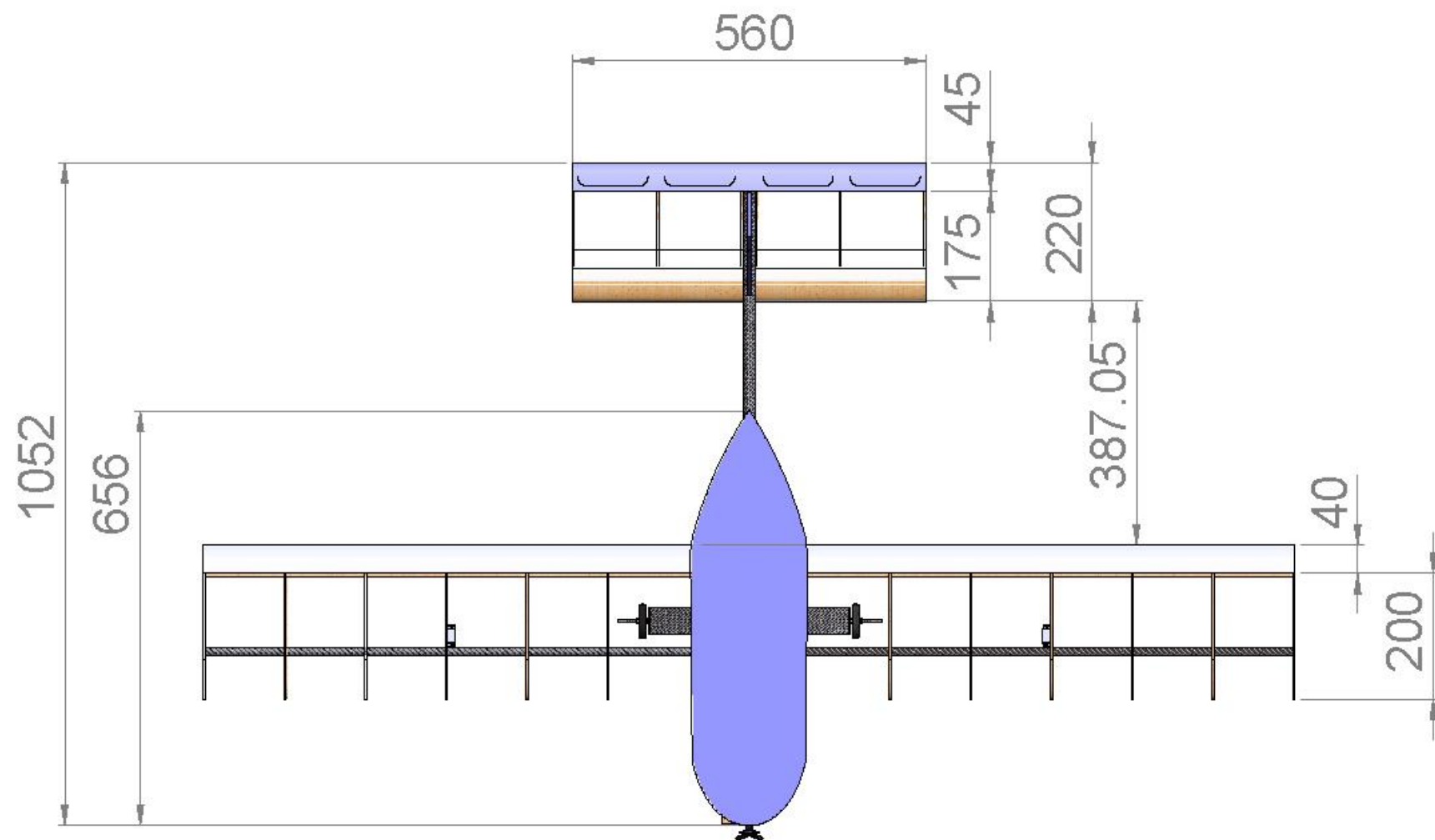
## 5.6 Predicted Mission performance

Table 5.8: Predicted Mission Performance.

MISSION PARAMETERS	M1	M2	M3
Empty Weight (lbs)	4.01	4.04	4.01
TOGW (lbs)	4.01	9.04	4.61
Number of servos	5	5	5
RAC (max)	20.05	20.2	20.05
Number of laps	6	NA	NA
Time to cover 3 laps (s)	NA	127	NA
Number of balls	NA	NA	4
Mission score	1.33	3.15	3.00
Flight score		7.48	
Flight score/ RAC <sub>max</sub>		0.37	

The performance of baseline aircraft considered for the calculation of the flight score in the above table is highly idealistic. Maximum number of laps for Mission 1 is assumed to be 9. Least time for the completion of Mission 2 is considered to be 100 seconds. Maximum number of balls dropped in mission 3 is assumed to be 8. The program estimated the empty weight of the aircraft as 3.6lb. However, the team is capable of manufacturing prototype weighing 4lb, and will continue to develop lighter prototypes.

## 5.7 Drawing Package



**SolidWorks Student Edition.  
For Academic Use Only.**



RASHTREEYA VIDYALAYA COLLEGE OF ENGINEERING

AIAA DESIGN/BUILD/FLY 2014/2015



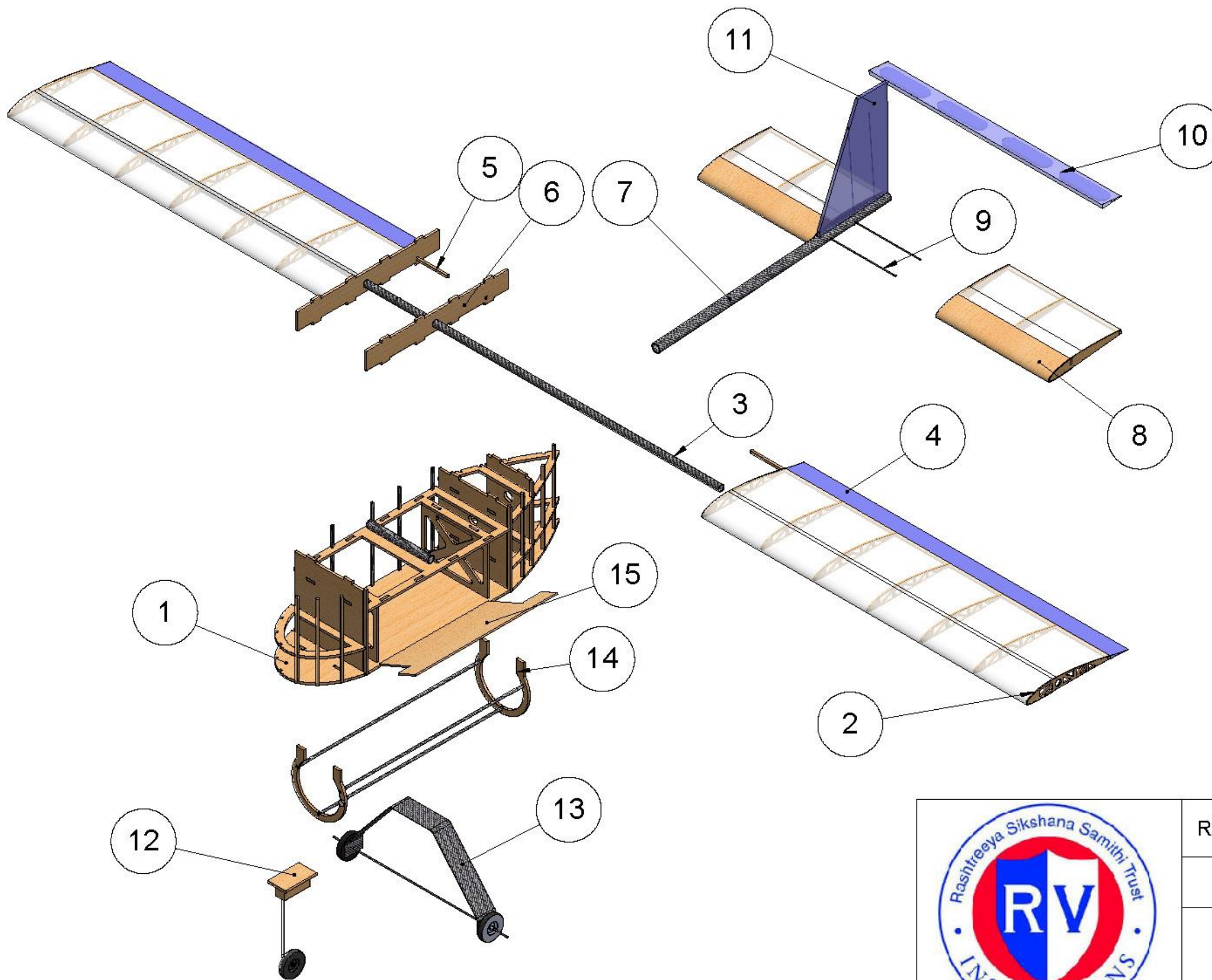
DRAWN BY: ANIRUDH.S

3 VIEW DRAWING

DIMENSIONS IN mm

SCALE 1:10

DATE: 02/16/2015



	Part	Material	Quantity
1	Fuselage	Balsa	1
2	Wing rib	Balsa	14
3	Main spar	Carbon tube	2
4	Flaperon	Balsa	2
5	Longeron	Balsa	2
6	Wing support	Balsa	2
7	Boom	Carbon tube	1
8	Horizontal tail	Balsa	2
9	Tail support	Carbon rod	4
10	Elevator	Balsa	1
11	Vertical tail	Balsa	1
12	Nose landing gear	Balsa, steel strut	1
13	Main landing gear	carbon fibre	1
14	Mission 3 structure	Balsa, carbon tubes	1
15	Hatch door	Balsa	1

**SolidWorks Student Edition.  
For Academic Use Only.**



RASHTREEYA VIDYALAYA COLLEGE OF ENGINEERING

AIAA DESIGN/BUILD/FLY 2014/2015



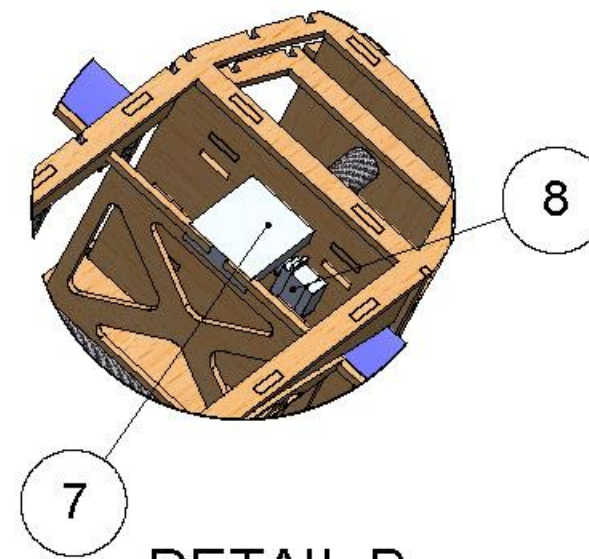
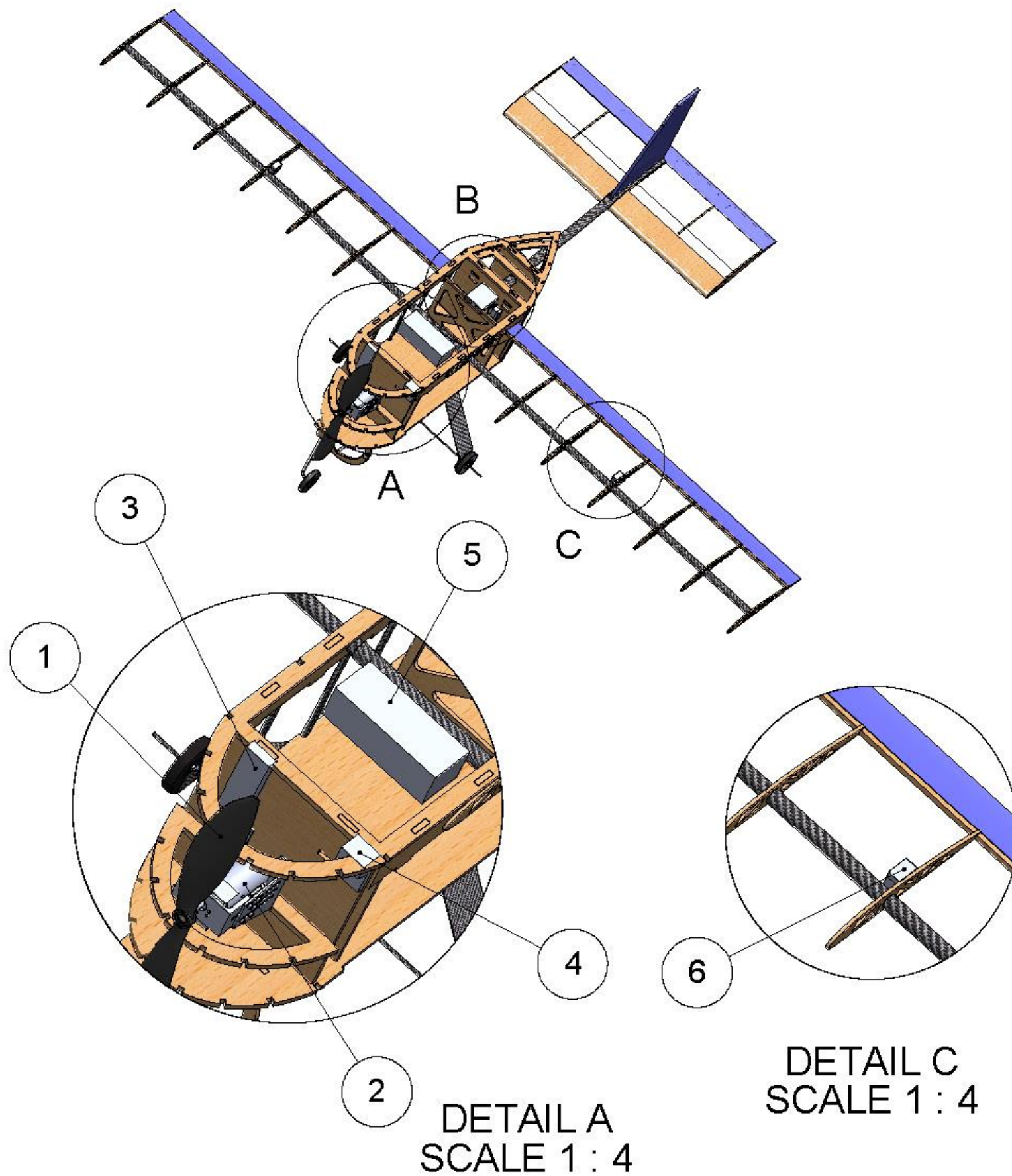
DRAWN BY: ANIRUDH.S

STRUCTURAL ARRANGEMENT

DIMENSIONS IN mm



SCALE 1:10

DATE: 02/16/2015

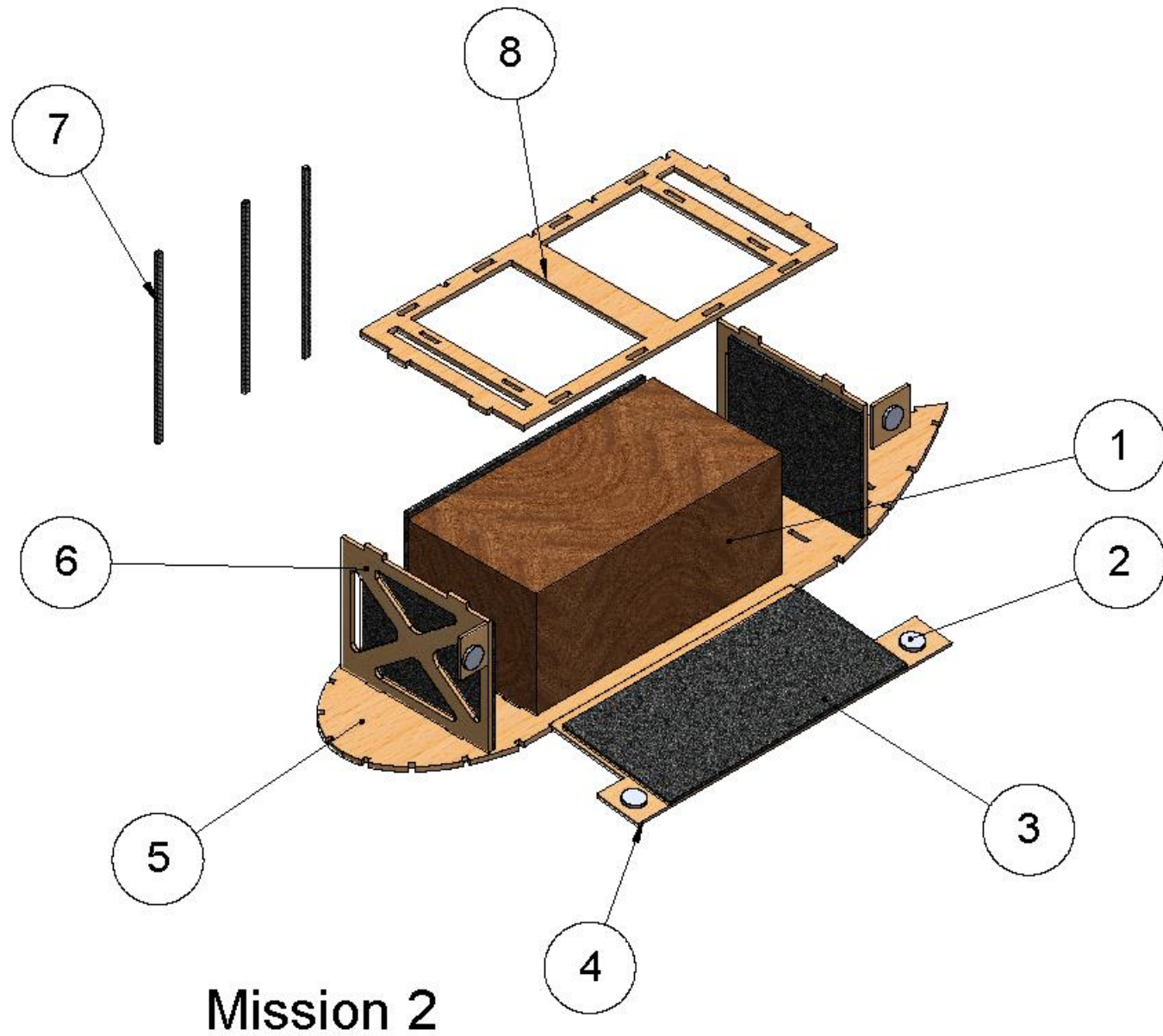


DETAIL B  
SCALE 1 : 4

	Part	Manufacturer	Model
1	Propeller	Master Airscrew	13x10
2	Motor	Electrifly	Ammo inrunner
3	Speed controller	Power HD	50A SBEC
4	Receiver	Flysky	I6
5	Main Battery	Elite	2000mah AA
6	Flaperon servo	Emax	12g ES08MD
7	Receiver Battery	Turnigy	400mah AA
8	Elevator servo	Emax	12g ES08MD

	RASHTREEYA VIDYALAYA COLLEGE OF ENGINEERING	
	AIAA DESIGN/BUILD/FLY 2014/2015	
		
DRAWN BY: ANIRUDH.S	SUB SYSTEMS CONFIGURATION	
DIMENSIONS IN mm	SCALE 1:10	DATE: 02/16/2015

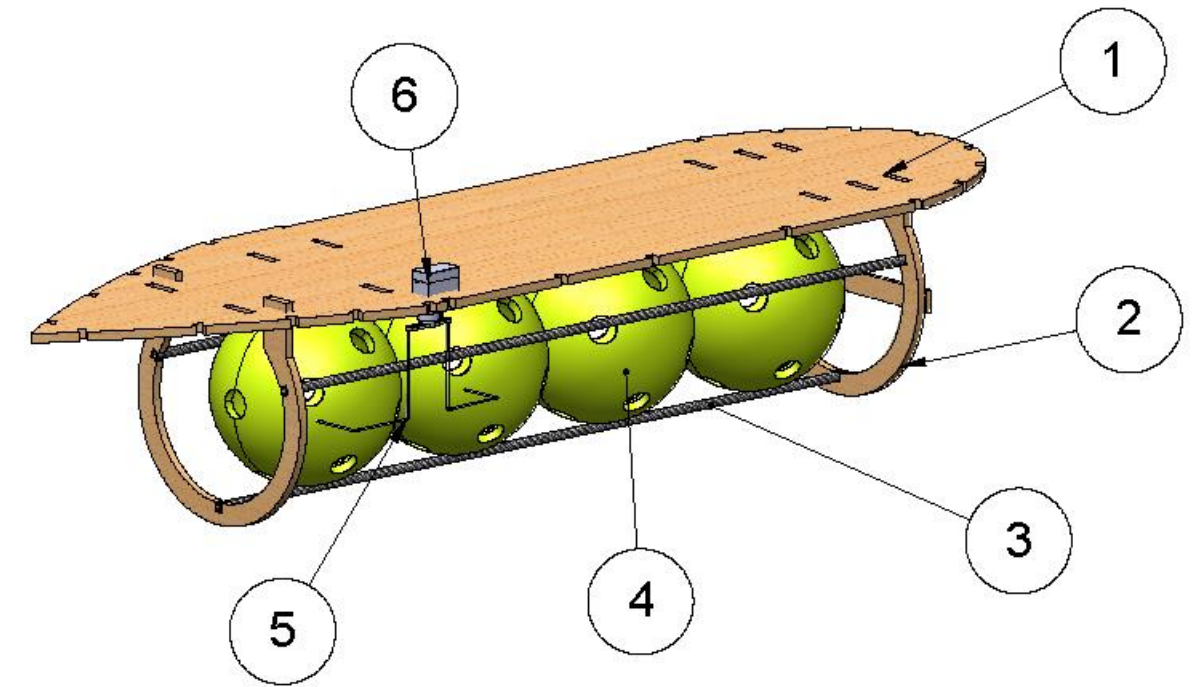
**SolidWorks Student Edition.  
For Academic Use Only.**



Mission 2



ITEM	COMPONENT
1	Payload - 2.2kg
2	Neodymium magnets
3	Sponge- payload restraint
4	Payload door
5	Fuselage bottom
6	Payload support
7	Carbon rod- stringers
8	Fuselage center piece

**SolidWorks Student Edition.  
For Academic Use Only.**



Mission 3

ITEM NO.	COMPONENT
1	Fuselage bottom
2	Balsa rings
3	Carbon fibre rods
4	Champro balls
5	C-shaped rod
6	Turnigy 9g servo

	RASHTREEYA VIDYALAYA COLLEGE OF ENGINEERING	
	AIAA DESIGN/BUILD/FLY 2014/2015	
		
DRAWN BY: ANIRUDH.S	PAYLOAD ACCOMODATION	
DIMENSIONS IN mm	SCALE 1:4	DATE: 02/18/2015

## 6 MANUFACTURING PLAN AND PROCESS

The goal of this phase is to manufacture a working model of the design. Incorporating the appropriate manufacturing techniques enables timely production of aircrafts, and eases the process of design alterations. The team's manufacturing choices were to some extent limited by the available equipment. The team adopted an iterative approach in arriving at the optimal prototype. First prototype was developed to validate the results of preliminary design. Later prototypes went on to test the readiness in completing missions. The final iteration encompassed weight optimization and drag reduction.

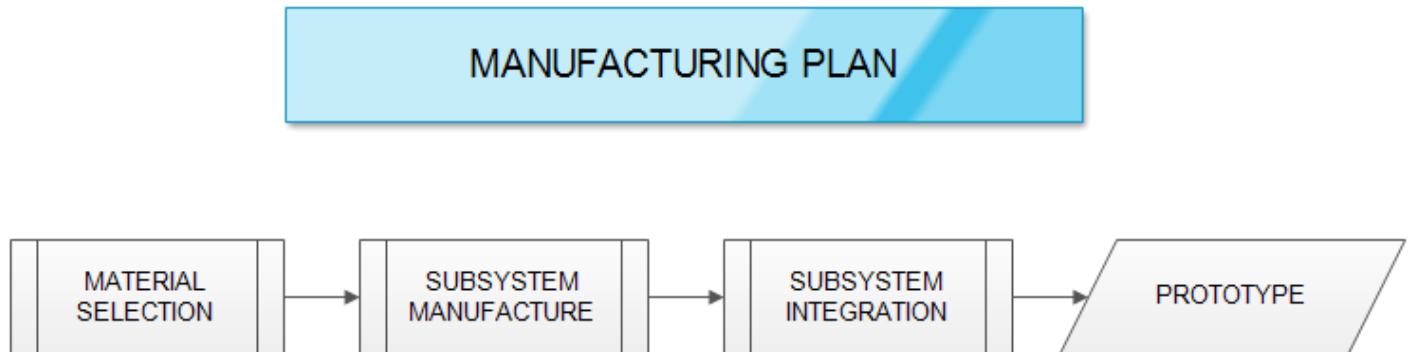


Figure 6.1: Manufacturing Plan Flowchart

### 6.1 Manufacturing and Material Selection

The team considered various feasible alternatives under material selection. It is vital to select the right material, which minimizes weight and ensures structural integrity. Manufacturing methods considered are as follows.

#### 6.1.1 Balsa Build Up

Balsa wood's low density allows for very light structures. However, its Strength to Weight ratio is significantly lower than that of composites. The team has a substantial amount of experience with balsa structures, which facilitates more complex build-ups.

#### 6.1.2 Composites

Composite structures are a popular choice due to their very high strength to weight ratios. Carbon fiber and Kevlar based composites have widely featured in this domain. However, composite structures are generally stronger than necessary except for the most limiting cases. Composite structures pose fabrication difficulties, especially for complex contours.

#### 6.1.3 Foam

Foam structures are convenient for their ease of manufacture. They are generally heavier than balsa build-ups, but they can also be made extremely light when used in non-loaded cases. Care must be taken with foam to use proper adhesives to avoid degradation.

#### 6.1.4 Balsa with Composites

Composites, when used to reinforce a balsa build up, have the advantage of providing higher strength in critical regions along with being lightweight. Structures made of balsa and composites have more durability which overshadows the demerit of escalation of manufacturing time.

### 6.1.5 Balsa and Foam


It is a common practice to build R/C aircrafts comprising of both Foam and Balsa build ups. Foam facilitates ease of manufacturing while balsa helps in making the plane light.

The judging criteria for material selection are as follows:

- **Weight:** Structural weight is an inversely related to the Overall Score. Hence, it is given the maximum weightage.
- **Strength:** All structural elements must be capable of resisting forces they are subjected to, with a factor of safety.
- **Ease of manufacture:** Familiarity and availability are significant aspects pertaining to manufacture.
- **Reparability:** Higher reparability is essential for quick rectification of defects, and is crucial to counter unforeseen hitches at the event.

The following table shows the trade-off amongst the available choices and the evaluating criteria.

Table 6.1: Material Decision Matrix

		Foam	Balsa	Carbon Fibre	Balsa + Carbon Fibre	Foam + Balsa
		Norm Rating	Norm Rating	Norm Rating	Norm Rating	Norm Rating
<b>Requirements</b>	<b>Norm Weighting</b>					
Weight	0.35	1	5	2	4	3
Strength	0.30	2	1	5	4	3
Repairability	0.20	1	5	2	4	3
Ease of Manufacture	0.15	5	4	1	2	3
<b>Grand Total</b>		<b>1.90</b>	<b>3.65</b>	<b>2.75</b>	<b>3.70</b>	<b>3.00</b>

## 6.2 Subsystem Manufacturing

### 6.2.1 Wing

Wing comprises of laser-cut balsa ribs and carbon tubes. The alignment of ribs at accurate positions was ensured by keeping to-scale plan of the wing underneath it and also by using assembly supports.

Laser cut ribs allowed for precise positioning of the two spars: a 14mm OD 12mm ID hollow carbon tube and a 5mmx5mm balsa spar. Torsional stiffness to the wing was provided by covering the leading edge with 1mm balsa sheet. Microlite® was used to cover the wing. It is the lightest option available, and has a higher Strength to Weight ratio when compared to Monokote or Vinyl. Further, weight can be reduced by providing lightening holes in the laser cut ribs and control surfaces. Half wings were first manufactured and then attached to the fuselage.

### 6.2.2 Fuselage and Payload Mounting System

Being an out-station team, it is required for the fuselage to be readily assembled in short lead times. Balsa wood of appropriate thickness is laser cut, and assembled in the form of a jig saw puzzle. Laser cutting provides for shorter manufacturing time, flexibility in cutting complex contours and quicker assemblies. Carbon fiber is used at strategic regions, which demand higher structural capabilities, while the motive remains to make the aircraft as light as possible, yet robust. The empennage is to be mounted at -4 degrees with respect to the horizontal, hence relevant fixtures were

readied to ensure the desired inclination. Cyanoacrylate glue, balsa strengthening coating (epoxy) and cross grain 1 mm balsa strips are used to reinforce at junctions and other weak links. Bulkheads are positioned to constrain the payload and to accommodate the elevator servo. A door is provided on the side of the fuselage to access the 5-lb payload. The door is hinged to the bottom of the fuselage, and neodymium magnets enable quick opening and closing of the door. The mechanism for external payloads is integrated with the base of fuselage. The necessary members are laser cut and machined as per requirement.

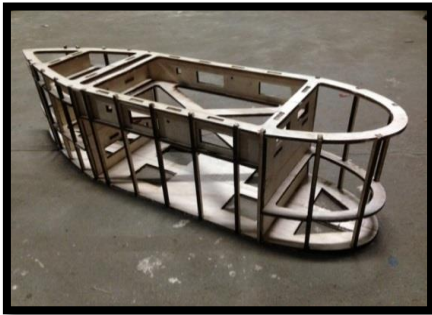


Figure 6.2: Fuselage Structure



Figure 6.3: External Payload Mounting

### 6.2.3 Empennage

Empennage includes the vertical stabilizer, the horizontal stabilizer and a boom. The carbon fiber boom comprises of 20mm diameter tube which is adequate to bear the loads exerted by the tail. Horizontal Tail is constructed using laser cut balsa ribs, which are connected by 5mm x 5mm spars, and a 2mm diameter carbon rod. Like the wing, the leading edge of the horizontal stabilizer is covered with 1mm water wetted balsa sheets. This gives it the required stiffness.

Flat plate vertical tail was also laser cut, which ensured dimensional accuracy. Grooves were made in two laser cut balsa sheets to accommodate two carbon rods which are sandwiched between them.

The carbon rods protruding out of the Horizontal stabilizer and Vertical stabilizer are made to pass through pre made holes in the boom. Fine adjustments, before gluing both the stabilizers to the boom, are crucial. Microlite® was used to cover the vertical and horizontal stabilizers.



Figure 6.4: Empennage Structure

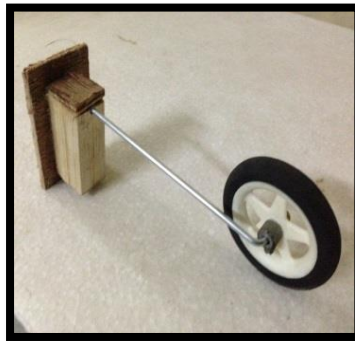


### 6.2.4 Landing Gear

The nose landing gear was fabricated out of 3mm mild steel rod. The rod was bent into an inverted U shape at one end, which was made to pass through a 20mm x 40mm x 20mm balsa piece to distribute the point load during landing (as shown in figure 6.5 a & b). A plywood piece was glued to the balsa piece which is attached to the fuselage.



(a) Hammering Process



(b) Nose Landing Gear



(c) Main Landing Gear

Figure 6.5: Landing Gear

The rear landing gear was made of carbon fiber reinforced polymer. Wooden male and female molds were cut using a band saw in the shape of landing gear. Carbon gets its strength from the direction of its fibers. In order to build a composite that is stiff from any angle, alternate cutting of the carbon fiber, straight and on the bias, at a 45-degree angle to the weave direction is employed. 4 layers of 200gsm carbon fiber layers were used. Carbon fiber was laid up in the mold using wet layup method and pressure was applied by using a vice. The two ends of the landing gear are connected by a carbon fiber rod to provide structural rigidity as shown.

### 6.3 Structural Integration

This section discusses about the assembly of sub-components – Wing, Fuselage, Empennage and Landing gear. Since the plane has to be transported internationally, the time for assembly before the competition is minimal. Keeping this in mind, the team has tried to reduce assembly time by using suitable manufacturing techniques. The boom is fixed to the fuselage by passing it through the holes in bulkheads and securing it with saw dust and CA glue. Front landing gear was fixed using araldite and hardener. Rear landing gear is positioned and screwed to the fuselage bottom, where a single layer of reinforcing carbon fiber plate was attached. Washers are used to uniformly distribute the pressure.

Wing attachment is one of the most critical parts of our integration process. Fuselage has two holes, one circular hole of 16mm diameter and other 5mm x 5mm square. A carbon rod of OD 16mm and ID 14mm is passed through these holes and is glued to the fuselage. The 14mm spars which extend out of the wing pass through the holes in the fuselage exactly to half its width. The main spar was secured using a hole-pin mechanism.

The motor was fixed using an aluminum motor mount which was screwed to the front bulk head. All the electronic components and wirings done are secured by adhesive tapes. The mandatory arming switch is placed on the outer side of the fuselage to make it easily accessible.

The mission 2 payload access door, made out of balsa, is hinged to the fuselage using hinge paper. Flaperons and elevator are fixed to wing and horizontal tail respectively using hinge paper. Finally covering of the fuse is done using Microlite®.



Figure 6.6: Half-wing Mounting



Figure 6.7: Empennage Integration with Fuselage

## 6.4 Prototype Evolution

Unidirectional Polycarbonate sheets were used to manufacture the first prototype, to test the design as this material is very durable. The second prototype was built completely using Balsa wood. In the third prototype, the fuselage was covered by 1mm water wetted balsa sheets. This was later changed to Microlite® in fourth and final prototype.



(a) VYOMA I



(b) VYOMA II



(c) VYOMA III



(d) VYOMA IV

Figure 6.8: Prototype Evolution

## 6.5 Manufacturing Milestone chart

In order to excel in the competition, proper manufacturing schedule plays a key role. Figure 6.8 shows the manufacturing schedule.

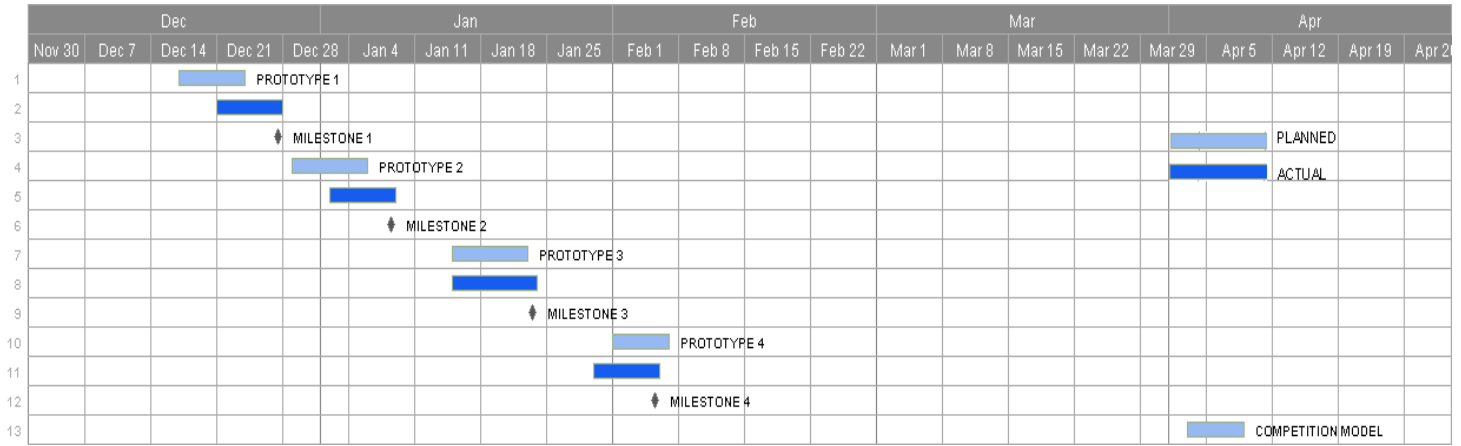


Figure 6.9: Manufacturing Milestone Chart

## 7 TESTING PLAN

### 7.1 Testing Objectives

The objective of the testing phase is to determine whether the aircraft and its various subsystems are capable of operating within the theoretical values. A series of tests are performed on the various components of the aircraft. From the conclusions drawn from the individual subsystem tests, design decisions are made and integrated into the aircraft assembly. The flowchart indicates the processes involved in this phase. FailType object determines the reason for failure, and loops to that particular phase for correction.

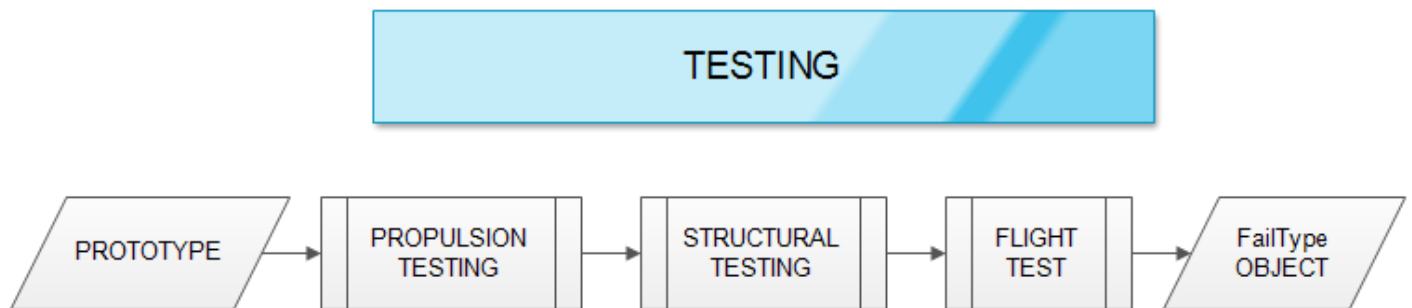


Figure 7.1: Testing Flowchart

### 7.2 Propulsion Testing

Propulsion system testing is performed to confirm the theoretical predictions and to validate manufacturers' data. In order to measure the thrust developed by different motor propeller combination, a thrust rig was built by the team. The thrust developed by the motor is transferred by the L-bracket onto a weighing scale. Figure 7.2 shows the thrust rig used by the team.

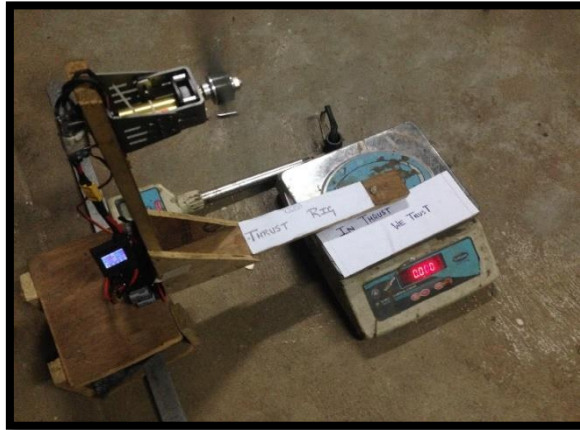


Figure 7.2: Motor Thrust Rig

Before the test flights, maximum current that can be drawn was measured during the thrust test. This was accomplished using a wattmeter. Also, the endurance of the battery was tested by operating the motor at 80% throttle.

### 7.3 Structural testing

Structural tests were conducted on two main sub-systems of the aircraft: Wing and Landing gear. Whiffletree test and wing tip test were conducted on the wing, whereas Static and dynamic loading tests were conducted on the landing gear. These tests confirm the predictions of SolidWorks® analysis conducted earlier.

#### 7.3.1 Wing

##### 7.3.1.1 Wing tip test

To simulate practical conditions during testing, the team decided to conduct the wing tip test on a prototype. Two team members held the plane at the wing tips and the plane was gradually loaded. The setup was tested until failure of the structure.



Figure 7.3: Wing Tip Test

##### 7.3.1.2 Whiffletree test

A half-wingspan test section was assessed using a whiffletree weight distribution with the root fixed. Whiffletree test relates a distributed loading condition to a single equivalent concentrated force of specific magnitude and location. The accuracy of the test increases as the number of levels in the whiffletree increases. The test setup is demonstrated below.



(a) Unloaded Condition

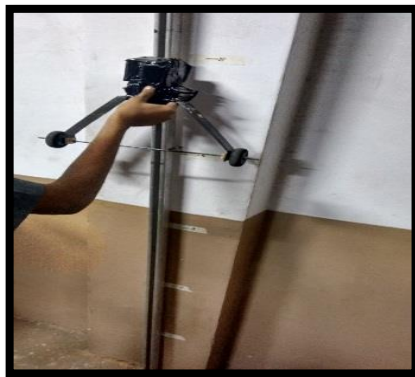


(b) Loaded Condition

Figure 7.4: Wiffletree Test

### 7.3.2 Landing gear

The Main landing gear was subjected to two tests: static load test and dynamic drop test. In the static load test the main landing gear was loaded with design load to validate the strength. In the dynamic drop test, is shown in Figure 7.5.



(a) Dynamic Test Setup (b) Static Test

Figure 7.5: Landing Gear Test

### 7.3.3 Door Test

Mission 2 payload is accessible by a magnet appended door, which is hinged to the fuselage. It was important to perform load test on this door to decide the size of the magnets. Test was conducted on a similar static structure by loading it gradually. Magnet detachment load was noted for different sized magnets and the magnet arrangement corresponding to a load of 1.8 kg per pair of magnets which matches the load on the door, when the plane is rotated by 90 degree about the roll axis, was selected.

## 7.4 Ground Mission Test

This competition year being the first time that Ground mission score is relative, the team decided on extensive testing in this domain. Groups of 3, performed the complete ground mission, and their respective times were noted. Based on the performance of the individuals, the final group was decided. Extensive practice is in process to minimize the mission time second by second.

## 7.5 Payload Drop Testing

The Mission 3 payload drop test was conducted in the windmill setup available in the college. The dropping of ball was performed at wind speeds equal to cruise velocity of mission 3.

## 7.6 Flight testing

### Take off test

A test for take-off distance was conducted to meet the given requirement of 60 ft., the distance 60 ft. was marked on the runway.



Figure 7.6: Successful Take-off of VYOMA IV

## 7.7 Planned Testing Schedule

Figure 7.7 displays the timing of planned and actual testing events leading up to competition.

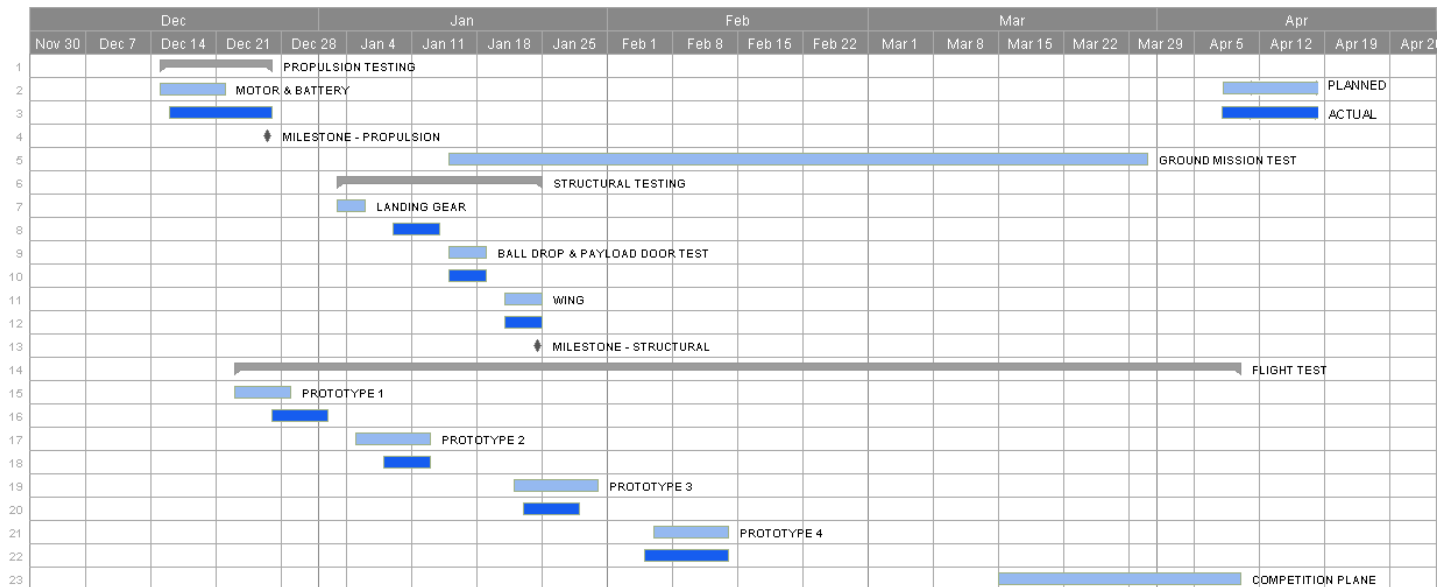


Figure 7.7: Testing Milestone Chart

## 7.8 Pre-flight Checklist

### 7.8.1 Tools and Support Equipment

Table 7.1: Tools and Support Equipment

TAPES	CUTTING TOOLS	OTHERS	
<input type="checkbox"/> Duct Tape	<input type="checkbox"/> X-acto Blades	<input type="checkbox"/> Balsa for repair	<input type="checkbox"/> Measuring Tape
<input type="checkbox"/> Masking Tape	<input type="checkbox"/> Wire Cutter	<input type="checkbox"/> Zip-tag	<input type="checkbox"/> Scale
<input type="checkbox"/> Paper Tape	<input type="checkbox"/> Scissors	<input type="checkbox"/> Foams	<input type="checkbox"/> Marker
<input type="checkbox"/> Clear Tape	<input type="checkbox"/> Hammer	<input type="checkbox"/> Carbon Fiber Rod	<input type="checkbox"/> Chalk
<input type="checkbox"/> Fiber Glass Tape	<input type="checkbox"/> Plier	<input type="checkbox"/> Spare Propellers	<input type="checkbox"/> Control Rod
<input type="checkbox"/> Insulation Tape	<input type="checkbox"/> Blades	<input type="checkbox"/> Battery Charger	<input type="checkbox"/> Screw-driver Set
<input type="checkbox"/> Double-sided Tape	<input type="checkbox"/> Hack Saw		

### 7.8.2 General Aircraft Checklist

- Aircraft structural Integrity: Visual inspection for damaged parts
- Avionics: Ensure all wires are firmly connected and components work as needed
- Propulsion: Ensure propulsion is all GO
- Final Inspection: Ensure safe flight

Table 7.2: Pre-flight Checklist

AIRCRAFT STRUCTURAL INTEGRITY			AVIONICS	PROPULSION	FINAL INSPECTION
<input type="checkbox"/> Propeller	<input type="checkbox"/> Payload drop Mechanism	<input type="checkbox"/> Motor	<input type="checkbox"/> Servo Wiring	<input type="checkbox"/> Battery Charge	<input type="checkbox"/> Ground Crew Clearance
<input type="checkbox"/> Boom	<input type="checkbox"/> Payload	<input type="checkbox"/> Landing Gear	<input type="checkbox"/> Range Test	<input type="checkbox"/> Motor Wiring	<input type="checkbox"/> Pilot & Spotter Ready
<input type="checkbox"/> Wing	<input type="checkbox"/> Fuselage	<input type="checkbox"/> Control Surfaces	<input type="checkbox"/> Fail-safe		<input type="checkbox"/> Final Visual Inspection
<input type="checkbox"/> Tail	<input type="checkbox"/> Nose Landing Gear		<input type="checkbox"/> Transmitter Battery		

## 8 PERFORMANCE RESULTS

The following section discusses the performance results obtained during testing. Extensive testing was done in each subsystem and the results were tabulated for comparison.

### 8.1 Propulsion

The propulsion predictions from V\_Design were tested to further calibrate the model. Static test results in Table 8.1 show that the propulsion model overestimated the static thrust values roughly by 15%. However, test flights proved that the chosen propulsion system was able to satisfy all the mission requirements.

Table 8.1: Propulsion Performance Results

PROPELLER		THRUST (lbs)		CURRENT (A)	
Dimensions	Mission	Predicted	Measured	Predicted	Measured
13X10	Mission 1	5.07	4.25	20.4	20.9
14X8	Mission 2	5.73	5.22	26.1	26.4
13X6.5	Mission 3	4.63	4.05	24.3	24.7

### 8.2 Structure

#### 8.2.1 Wing test

Two tests were conducted on the wing – Wingtip test and Whiffletree test. At 4kg (which is the expected Mission 2 gross weight) the wing didn't suffer any damage. In order to obtain the failure load, the plane was loaded further gradually. At a weight of 7kg the structure failed, roughly corresponding 6G load. It was observed that the root of the wing was the stress concentrated region and thus the team decided to reinforce the same. The result of the whiffle tree test are tabulated as below. Considering a factor of safety 3, the half wing was subjected to gradual bending load up to 6Kg. Table 8.2 shows the wing deflection for various loads. This test ensured structural strength of the wing.

Table 8.2: Whiffletree Test Performance Results

LOAD (lbs)	DEFLECTION (in)	CONDITION
4.4	0.6	SAFE
8.81	1.3	SAFE
13.22	1.8	SAFE

#### 8.2.2 Landing gear

The main landing gear was subject to two tests that ensured its reliability: a static loading test and a Dynamic drop test. The static loading test comprised of loading the main landing gear up to failure. The failure occurred at a load of 17.6kg which is more than 4 times the maximum gross weight of the plane. The failure occurred in the region as predicted by the SolidWorks® analysis earlier. Dynamic drop test was conducted by fixing the main landing gear to a stand. Loading the gear to 4kg and dropping from a height of 4ft helped simulate hard landing and stalled landing.





Figure 8.1: Landing Gear Failure after Static Loading Test

### 8.3 Flight performance

The V\_Design, tailor-made for this year's competition, provided the theoretical targets which the fabricated prototypes had to adhere to. Flight tests were performed to accurately mimic the missions. The course was chalked out with accurate measurements and markers were placed to define the boundaries.

The goal of testing was to identify the inconsistencies in the prototypes, and to compare flight performance with predicted performance. Also, extensive testing would enable the team to know the complete capabilities of the prototypes, and allow the team to gauge the influence of minor changes in design such as control surface sizing, span increments/decrements on performance.

The first prototype, VYOMA-I failed to take off. Upon examination, improper positioning of the Landing gear was found to be the cause of failure. The team rectified the calculation error, and incorporated the same in the subsequent flights.

The second prototype, VYOMA-II took off successfully, but upon landing, the nose landing gear collapsed, and the fuselage could not bare the impact, and shattered. This called for proper fixing techniques for the nose landing gear. Carbon fiber reinforcement was provided at sections subjected to impact loads. Since the major structural failures were addressed in the first two test flights, the agenda thereafter was to test the mission readiness of the plane.

The third prototype, VYOMA-III was successful in completing the course with the internal payload, but an error in piloting caused it to plummet into a nearby tree.

The fourth prototype, VYOMA-IV was successful in meeting all the mission requirements. The focus after the fourth prototype was to extract the best Overall Competition Score. This included resizing control surfaces, span, weight reduction and repeated testing.

#### 8.3.1 Flight Logbook

It is a tradition of the team to maintain a Flight Logbook which contains detailed information of every flight. This documentation is very helpful in analyzing the errors and preventing the same in subsequent flights. Table 8.3 shows the logbook entries of DBF 2014-15 test flights.

Table 8.3: Flight Logbook

NAME	DATE	DESCRIPTION	REMARKS
<b>VYOMA I</b>	27/12/2014	Uni-directional polycarbonate sheet build up.	Failed to take off.
<b>VYOMA II</b>	05/01/2015	Balsa build up	Crash during landing.
<b>VYOMA III</b>	22/01/2015	Balsa+carbon fiber build up	Successful take-off, crashed tree.
<b>VYOMA IV</b>	06/02/2015	Balsa+carbon fiber build up	Successful performance of all missions.

Table 8.4: Comparison of predicted and demonstrated flight performance

MISSION	SCORING PARAMETER	PREDICTED	DEMONSTRATED
<b>Mission 1</b>	#Laps	6	6
<b>Mission 2</b>	Time for 3 laps (s)	127	144
<b>Mission 3</b>	#Balls	4	4

Given the results of the completed tests, the team believes it can put up a commendable performance as a debutant at the 2014/15 competition. Burning the midnight oil and mosquito coil has been the norm over the past few months, to ensure that the team fulfills its potential. The journey has been fun and fulfilling, and the experience has been truly memorable.



Figure 8.2: VYOMA IV Successful Flight.

## 9 REFERENCES

1. AIAA Student Design/Build/Fly, "DBF Rules," 31 October 2014. [Online]. Available: [http://www.aiaadb.org/2015\\_files/2015\\_rules\\_final\\_20141031.html](http://www.aiaadb.org/2015_files/2015_rules_final_20141031.html)
2. J. D. Anderson Jr., Introduction to Flight, 7th ed. New York: McGraw Hill, 2007.
3. Genetic Algorithm Documentation, The MathWorks Inc., Natick, MA, 2014;
4. "UIUC Airfoil Coordinates Database," University of Illinois at Urbana-Champaign Department of Aerospace Engineering, [Online]. Available: [http://www.ae.illinois.edu/m-selig/ads/coord\\_database.html](http://www.ae.illinois.edu/m-selig/ads/coord_database.html).
5. "APC Propellers,". [Online] Available: <http://www.apcprop.com>
6. Drela .M, DC Motor/Propeller Matching. [online]. Available : [web.mit.edu/drela/Public/web/qprop/motorprop.pdf](http://web.mit.edu/drela/Public/web/qprop/motorprop.pdf)
7. "NASA Systems Engineering Report". SAE Aero Design® West Competition. R.V. College of Engineering, 2013.
8. Mohammad H. Sadraey (2013). Aircraft Design, A Systems Engineering Approach. [online]. Available: [faculty.dwc.edu/sadraey/Chapter%209.%20Landing%20Gear%20Design.pdf](http://faculty.dwc.edu/sadraey/Chapter%209.%20Landing%20Gear%20Design.pdf)
9. Dynamic equations of Flight Vehicles. [online]. Available: [courses.cit.cornell.edu/mae5070/DynamicEquations.pdf](http://courses.cit.cornell.edu/mae5070/DynamicEquations.pdf)
10. Drela. M, and H. Youngren. XFLR5. Computer software. Available: <http://xflr5.sourceforge.net/xflr5.htm/>
11. Drela. M, and H. Youngren. AVL. Computer software. Available: <http://web.mit.edu/drela/Public/web/avl/>
12. MATLAB®. Vers. R2013a. Natick, MA: MathWorks, 2013. Computer software.
13. SolidWorks®. Vers. 2014 (Student Edition). SolidWorks® Corp., 2011. Computer software.